

Recycling of dental zirconia residuals resulting from CAD/CAM milling process

Submitted to the Graduate School of Natural and Applied Sciences
in partial fulfillment of the requirements for the degree of
Master of Science in Department of Materials Science and
Engineering

by

Merve TORMAN KAYALAR

ORCID 0000-0001-8679-622X

December, 2022

This is to certify that we have read the thesis **Recycling of dental zirconia residuals resulting from CAD/CAM milling process** submitted by **Merve TORMAN KAYALAR**, and it has been judged to be successful, in scope and in quality, at the defense exam and accepted by our jury as a MASTER'S THESIS.

APPROVED BY:

Advisor:

Prof. Dr. Mücahit SÜTÇÜ
İzmir Kâtip Çelebi University

Committee Members:

Assist. Prof. Dr. İsmail Doğan KÜLCÜ
İzmir Kâtip Çelebi University

Assoc. Prof. Dr. Mustafa EROL
Dokuz Eylül University

Date of Defense: December 16, 2022

Declaration of Authorship

I, **Merve TORMAN KAYALAR**, declare that this thesis titled **Recycling of dental zirconia residuals resulting from CAD/CAM milling process** and the work presented in it are my own. I confirm that:

- This work was done wholly or mainly while in candidature for the Master's degree at this university.
- Where any part of this thesis has previously been submitted for a degree or any other qualification at this university or any other institution, this has been clearly stated.
- Where I have consulted the published work of others, this is always clearly attributed.
- Where I have quoted from the work of others, the source is always given. This thesis is entirely my own work, with the exception of such quotations.
- I have acknowledged all major sources of assistance.
- Where the thesis is based on work done by myself jointly with others, I have made clear exactly what was done by others and what I have contributed myself.

Date: 16.12.2022

Recycling of dental zirconia residuals resulting from CAD/CAM milling process

Abstract

Pre-sintered zirconia blocks stabilized with 3 mol% yttria are the most widely used dental materials in dental prostheses due to their high mechanical strength, high oxidation and wear resistance, high hardness, and excellent biocompatibility. Thanks to the processing of dental blocks with the CAD / CAM process, aesthetic restorations with excellent precision and high surface quality can be produced. However, only 30% of the blocks processed during the CAD/CAM process can be converted into products, while some of the remainder turns into dust and is collected in filters, and the other part becomes inactive as processed waste blocks. Considering the financial value of zirconia, waste zirconia in specified amounts causes a serious economic loss. From an environmental and economic point of view, there will be obvious benefits from recycling this waste and reusing it as a high value-added material. With this motivation, in this thesis study, the recycling of dental zirconia block wastes formed after the CAD/CAM processing process and their reusability in dental applications were investigated.

Waste dental zirconia blocks, collected in sufficient quantity from a local dental laboratory, were pulverized and sieved below 45 μm . After the raw material characterization, the recycled dental zirconia powder was mixed with 3 mol% yttria added commercial zirconia powder in various proportions. After the prepared

compositions were formed into pellets, they were cold isostatically pressed (CIP) under 250 MPa pressure. The prepared samples were first pre-sintered at 1000°C for 4 hours and then fully sintered at 1450°C, 1500°C and 1550°C for 2 hours. The weight and dimensional changes of the obtained ceramic bodies were calculated. Phase analysis of the samples and tetragonal to monoclinic phase changes after aging test (LTD) were detected by X-ray diffraction (XRD). Morphological properties and grain sizes of raw materials and sintered samples were determined by scanning electron microscopy (SEM). Density measurements were carried out using the Archimedes' method. A number of mechanical tests (Vickers hardness, fracture toughness and three-point bending test) were applied to the sintered samples and the results were evaluated according to the sintering temperature and the addition of recycled zirconia powder. Comparing the findings with the samples produced entirely from commercial powder (COM) and the samples produced from the original block (OB) processed in CAD/CAM, inferences were made about the reusability of 3 mol% yttria added, pre-sintered waste dental zirconia blocks by recycling them in dental areas.

Comparing the findings with samples produced entirely from commercial powder (COM) and samples produced from the original block (OB) processed in CAD/CAM, inferences were made about the reusability of pre-sintered dental zirconia blocks with 3 mol% yttria added by recycling in dental fields.

Keywords: Dental zirconia block residuals, CAD/CAM processing, recycling dental zirconia, aging test, characterization, cold isostatic pressing

CAD/CAM işleme prosesinden elde edilen dental zirkonya atıklarının geri dönüşümü

ÖZ

%3 mol itriya ile stabilize edilen ön sinterlenmiş zirkonya bloklar, yüksek mekanik mukavemetleri, yüksek oksidasyon ve aşınma direnci, yüksek sertlikleri ve mükemmel biyouyumlulukları nedeniyle diş protezlerinde en yaygın kullanılan dental malzemelerdendir. Dental blokların CAD/CAM ile işlenmesi sayesinde mükemmel hassasiyet ve yüksek yüzey kalitesine sahip estetik restorasyonlar üretilebilmektedir. Ancak CAD/CAM işlemi sırasında işlenen blokların sadece %30'u ürüne dönüştürülebilirken, bir kısmı toza dönüşerek filtrelerde toplanmakta, kalan kısmı ise işlenmiş atık bloklar olarak inaktif hale gelmektedir. Zirkonyanın maddi değeri düşünüldüğünde, belirtilen miktarlardaki atık zirkonya, ciddi bir ekonomik kayba neden olmaktadır. Çevresel ve ekonomik açıdan bakıldığında, bu atıkların geri dönüştürülmesi ve katma değeri yüksek bir malzeme olarak yeniden kullanılmasının bariz faydaları olacaktır. Bu motivasyonla bu tez çalışmasında, CAD/CAM işleme süreci sonrasında oluşan dental zirkonya blok atıklarının geri dönüşümü ve dental uygulamalarda tekrar kullanılabilirliği araştırılmıştır.

Yerel bir diş laboratuvarından yeterli miktarda toplanan atık diş zirkonya blokları toz haline getirildi ve 45 µm'nin altında elendi. Hammadde karakterizasyonundan sonra, geri dönüştürülen dental zirkonya tozu, %3 mol itriya katkılı ticari zirkonya tozu ile çeşitli oranlarda karıştırılmıştır. Hazırlanan bileşimlere pelet forma getirildikten sonra

250 MPa basınç altında soğuk izostatik pres (CIP) uygulanmıştır. Hazırlanan numuneler önce 1000°C'de 4 saat ön sinterlenmiş, ardından 1450°C, 1500°C ve 1550°C'de 2 saat süre ile tam sinterlenmiştir. Elde edilen seramik bünyelerin ağırlık ve boyutsal değişimleri hesaplanmıştır. Numunelerin faz analizleri ve yaşlandırma testi (LTD) sonrasında numunelerde meydana gelen tetragonal-monoklinik faz dönüşümleri X-ışını kırınımı (XRD) ile tespit edilmiştir. Hammaddelerin ve sinterlenen numunelerin morfolojik özellikleri ile tane boyutları taramalı elektron mikroskobu (SEM) ile tayin edilmiştir. Yoğunluk ölçümleri Arşimed metodu ile gerçekleştirilmiştir. Sinterlenen numunelere çeşitli mekanik testler (Vickers sertliği, kırılma tokluğu ve üç nokta eğilme testi) uygulandı ve sonuçlar sinterleme sıcaklığına ve geri dönüştürülmüş zirkonya tozu ilavesine göre değerlendirildi. Elde edilen bulgular tamamen ticari tozdan üretilmiş numuneler (COM) ve CAD/CAM'de işlenmiş orjinal bloktan üretilen numuneler (OB) ile kıyaslanarak, %3 mol itriya ile stabilize edilen ön sinterlenmiş atık dental zirkonya blokların geri dönüştürülerek dental alanlarda yeniden kullanılabilirliği hakkında çıkarımlarda bulunulmuştur.

Anahtar Kelimeler: Dental zirkonya blok artıkları, CAD/CAM prosesi, dental zirkonyanın geri dönüşümü, yaşlanma testi, karakterizasyon, soğuk izostatik presleme

Acknowledgment

First and foremost, I would like to express my gratitude to my advisor, Prof.Dr. Mücahit Sütçü for his guidance and suggestions. Also, I would like to thank the members of my thesis supervising committee, Assoc. Prof. Dr. Mustafa Erol and Assist. Prof. Dr. İsmail Doğan Külçü for their technical support and comments.

I would like to thank my dear instructor Assoc. Prof. Dr. İlke Anaç Şakır from Gebze Technical University for her interest, politeness, patience, and support in the last year of my graduate program. I am also grateful to Gebze Technical University, Department of Materials Science and Engineering, and to Ahmet Nazım and Adem Şen from the staffs of department's laboratory, for their support for my laboratory studies. In addition, I would like to thank Atlas-Enta Dişçilik San. Tic. A.Ş. for their support in the laboratory studies during the production phase.

I would also like to thank my dear friends and colleagues Asst. Ahmet Yavaş and Asst. Dr. Saadet Güler for their support, help, cooperation and eternal friendship in my professional and social life.

Finally, I would like to special thank my beloved husband Aykut Kayalar and my precious family for their faith in me and their invaluable support. Despite all the difficulties I experienced, the successful completion of this work was made possible by their constant love and support.

This thesis was supported by İzmir Katip Çelebi University, Coordination Office of Scientific Research Projects (Project no: 2021-TYL-FEBE-0016).

Table of Contents

Declaration of Authorship.....	i
Abstract	ii
Öz.....	iv
Acknowledgment	vi
List of Figures	x
List of Tables.....	xiii
List of Abbreviations.....	xiv
List of Symbols	xv
1 Introduction	1
2 Literature Review.....	3
2.1 Zirconium oxide.....	3
2.2 Crystal Structure of Zirconia	5
2.3 Stabilization of Zirconia	6
2.4 Phase Diagram of ZrO_2 - Y_2O_3	7
2.5 Transformation Toughness Mechanisms	9
2.6 Low Temperature Degredation (Aging)....	11
2.7 Ceramic Powder Molding Methods	12
2.7.1 Uniaxial Dry Pressing.....	13
2.7.2 Isostatic Pressing	13
2.8 Sintering	15
2.9 CAD/CAM System	17
2.10 Recycling of Dental Zirconia Ceramics.....	19

3	Experimental Procedure	23
3.1	Materials	23
3.2	Method	25
3.2.1	Production of Samples.....	25
3.2.2	Pre-sintering and Sintering Processes.....	28
3.3	Characterization of Samples	29
3.3.1	Particle Size Analysis	29
3.3.2	Differential Thermal Analysis	29
3.3.3	Weight Loss and Dimensional Change Measurements	30
3.3.4	Optical Dilatometer	30
3.3.5	Density Measurements	31
3.3.6	Accelerated Aging Test	32
3.3.7	X-Ray Diffraction (XRD) Analysis.....	33
3.3.8	Scanning Electron Microscopy (SEM).....	33
3.3.9	Measuring Mechanical Properties	34
3.3.9.1	Microhardness	34
3.3.9.2	Indentation fracture toughness	35
3.3.9.3	Three-point Bending Test.....	36
4	Results and Discussion	38
4.1	Raw Material Characterization Results	38
4.1.1	Particle Size Distribution Results	38
4.1.2	Differential Thermal Analysis Results.....	39
4.1.3	Optical Dilatometer Results	40
4.1.4	XRD Analysis Results	42
4.1.5	SEM Results.....	43
4.2	Produced Samples Characterization Results.....	44
4.2.1	Weight Loss and Dimensional Change Analysis Results.....	44

4.2.2	Density Measurements Results	47
4.2.3	XRD Results	50
4.2.4	Accelerated Aging Test Results.....	53
4.2.5	SEM Results.....	57
4.2.6	Mechanical Test Results	60
4.2.6.1	Microhardness	61
4.2.6.2	Indentation Fracture Toughness	63
4.2.6.3	Three-point Bending Test.....	64
5	Conclusions	67
	References	70
	Curriculum Vitae	79

List of Figures

Figure 2.1	Crystal structures of zirconia polymorphs.....	5
Figure 2.2	Schematic representation of zirconium oxide and metal oxide binary phase diagram.....	7
Figure 2.3	Phase diagram of the ZrO_2 - Y_2O_3 system.....	8
Figure 2.4	Phases and fracture toughness values of zirconia according to yttria content.	8
Figure 2.5	A schematic representation of the transformation of zirconia grains in the stress field of the crack by stress [9].	9
Figure 2.6	Schematic illustration of martensitic tetragonal to monoclinic transformation.	10
Figure 2.7	Schematic representation of grinding-induced phase transformation in surface layers.....	10
Figure 2.8	The steps of the low-temperature degradation process	12
Figure 2.9	The schematic representation of the dry pressing method.	13
Figure 2.10	Cold isostatic press and application scheme.	14
Figure 2.11	Schematic diagram of stages and pore structures of solid-state sintering..	16
Figure 2.12	A schematic illustration of the microstructure changes during liquid phase sintering.....	17
Figure 2.13	Restored pre-sintered block after CAD/CAM milling process.	18
Figure 3.1	CAD/CAM machined pre-sintered zirconia block.....	23
Figure 3.2	Flow chart of the production steps of the samples.	26
Figure 3.3	Dry pressed samples.....	28
Figure 3.4	Pre-sintering and full-sintering schedule.....	28
Figure 3.5	Schematic representation of (a) dry weight, D , (b) suspended weight, S , and (c) saturated weight, W measurements according to Archimedes' principle.....	32

Figure 3.6	Schematic representation of the Vickers hardness measurement method and the shape of the trace.	35
Figure 3.7	A schematic representation of Vickers indentation and c, crack length.	36
Figure 3.8	Schematic representation of the three-point bending test setup.	37
Figure 4.1	Particle size distribution graphs of recycled zirconia powder (R-YSZ).	39
Figure 4.2	Particle size distribution graphs of commercial zirconia powder (COM).	39
Figure 4.3	TG-DTG curve of polyvinyl alcohol (PVA).	40
Figure 4.4	Optical dilatometer curves of a) COM, and b) R-YSZ.	42
Figure 4.5	XRD patterns of commercial zirconia powder (COM) and recycled zirconia powder (R-YSZ).	43
Figure 4.6	SEM micrographs of raw materials, a) COM, b) R-YSZ.	44
Figure 4.7	XRD patterns of samples sintered at 1450°C.	51
Figure 4.8	XRD patterns of samples sintered at 1500°C.	52
Figure 4.9	XRD patterns of samples sintered at 1550°C.	52
Figure 4.10	XRD patterns of samples sintered at 1450°C, 1500°C, and 1550°C, after aging process for 5h, 10h and 15h.	54
Figure 4.11	XRD patterns of samples sintered at 1450°C, 1500°C, and 1550°C, after aging process for 5h, 10h and 15h.	55
Figure 4.12	Percent monoclinic phase transformation of samples sintered at 1450°C, after aging process for 5h, 10h and 15h.	55
Figure 4.13	Percent monoclinic phase transformation of samples sintered at 1500°C, after aging process for 5h, 10h and 15h.	56
Figure 4.14	Percent monoclinic phase transformation of samples sintered at 1550°C, after aging process for 5h, 10h and 15h.	56
Figure 4.15	SEM images of OB, COM, and 3R-YSZ samples, a) OB-145, b) OB-150 c) OB-155, d) COM-145, e) COM-150, f) COM-155, g) 3R-YSZ-145, h) 3R-YSZ-150, j) 3R-YSZ-155.	57
Figure 4.16	SEM images of 5R-YSZ, 10R-YSZ and 15R-YSZ samples, a) 5R-YSZ-145, b) 5R-YSZ-150 c) 5R-YSZ-155, d) 10R-YSZ-145, e) 10R-YSZ-150, f) 10R-YSZ-155, g) 15R-YSZ-145, h) 15R-YSZ-150, j) 15R-YSZ-155.	58

Figure 4.17 SEM images of 30R-YSZ, 50R-YSZ and 100R-YSZ samples, a) 30R-YSZ-145, b) 30R-YSZ-150 c) 30R-YSZ-155, d) 50R-YSZ-145, e) 50R-YSZ-150, f) 50R-YSZ-155, g) 100R-YSZ-145, h) 100R-YSZ-150, j) 100R-YSZ-155.....	59
Figure 4.18 Microhardness values of sintered samples.	62
Figure 4.19 Indentation fracture toughness values of sintered samples.	64
Figure 4.20 Vickers indentation image of 5R-YSZ-145 sample.	64
Figure 4.21 Three-point bending strength and elastic modulus curves of all sintered samples.	65

List of Tables

Table 2.1	Properties of different ZrO ₂ products.....	4
Table 2.2	Crystal structure of pure zirconia	6
Table 3.1	Chemical composition and some physical properties of Upcera powder	24
Table 3.2	Chemical composition and some physical properties of Tosoh TZ-3YS-E powder.....	25
Table 3.3	Sample names and waste zirconia contents.....	27
Table 4.1	The linear shrinkage of samples.....	45
Table 4.2	The percent diameters change of samples.....	46
Table 4.3	The percent weight loss of samples.....	46
Table 4.4	The average dimensional volumes of samples.....	47
Table 4.5	Bulk density of pre-sintered and sintered samples.....	48
Table 4.6	Apparent specific gravity of pre-sintered and sintered samples.....	49
Table 4.7	Apparent porosity of pre-sintered and sintered samples.....	50
Table 4.8	Average grain sizes of sintered samples.....	59

List of Abbreviations

CAD	Computer-aided design
CAM	Computer-aided manufacturing
YSZ	Yttria stabilized zirconia
CIP	Cold isostatic press
HIP	Hot isostatic press
LTD	Low temperature degradation
PVA	Polyvinyl alcohol
SEM	Scanning electron microscopy
XRD	X-ray diffraction
TGA	Thermal gravimetry analysis
ISO	International Standards Organization
TZP	Tetragonal zirconia polycrystals
GPa	Gigapascal
IF	Indentation fracture
ASTM	American Society for Testing and Materials

List of Symbols

°	Degree
°C	Celsius degree
μm	Micro meter
nm	Micro meter
rpm	Revolutions per minute
%	Percent
t	Tetragonal phase
m	Monoclinic phase

Chapter 1

Introduction

Recently, zirconia-based ceramic restorations have taken the place of metal-supported ceramic restorations, which were frequently used in dental applications in the past, due to disadvantages such as thermal expansion difference, insufficient light transmission, the potential for oxide formation on the metal surface, allergic effects and aesthetic deficiencies [1]. Zirconia-based ceramic restorations stand out thanks to their high toughness and hardness values, biocompatibility and excellent aesthetic properties such as translucency, natural tooth color, and extraordinary light transmittance. There are three polymorphs of zirconia from room temperature to melting point. The polymorphic structure causes the tetragonal-monoclinic (t-m) phase transformation, which is a characteristic behavior specific to zirconia, and a volumetric change of 3-4% during this time. This phenomenon greatly limits the industrial applications of pure zirconia, which is unstable at room temperature. It has been discovered that the t-m phase transformation, occurring for various reasons in zirconium oxide, where the tetragonal phase is stabilized at room temperature by means of various oxides, can increase both the hardness and toughness properties of zirconia [2]. Zirconia stabilized with 3% mol yttria (3Y-TZP) is one of the most frequently used materials in dental fields with its high fracture toughness.

Yttria stabilized zirconia is brought into block form for use in dental applications. Ceramic blocks, which are pre-sintered to reach ideal hardness for ease of shaping, are processed with CAD/CAM for the production of restorations such as inlays, onlays, crowns and bridges, and converted into products. CAD/CAM systems are widely used in dentistry because they shorten the construction process of restorations and enable the production of standard quality, high precision, aesthetic restorations. In addition to its advantages, it causes a significant amount of wastage of the processed blocks during

CAD/CAM systems. In fact, only 30% of the blocks processed during the CAD/CAM process can be converted into products. Considering this amount, the disposal of zirconia, which is a high-cost material, is a significant economic and environmental damage.

The aim of this thesis is to recycle the machined zirconia blocks discarded after processing in dental laboratories by pulverizing them in certain sizes, and to investigate their reusability as a material with high added value in dental fields. For this purpose, recycled zirconia was mixed with commercial zirconia powder with the same properties in various proportions. It was deduced about the samples produced from the prepared compositions in terms of dimensional changes, density, microstructure, phase content, artificial aging and mechanical properties by comparing them with the samples obtained entirely with commercial powder and the standards defining usability in dental areas. In Chapter 3, the processes applied for the recycling of waste zirconia blocks, the production processes of the samples and the characterization methods are explained in detail. After the analysis and measurements made on the samples produced in Chapter 4, the obtained findings were examined in detail. The results were often shared as tables and graphics, and interpreted by comparing them with the findings in the literature. In Chapter 5, the findings were summarized and various suggestions were made for future studies.

Chapter 2

Literature Review

2.1 Zirconium oxide

Zirconium, a word derived from the Persian word "zargun" meaning "like gold", was first discovered in 1789 by the German chemist Martin Heinrich Klapoth [3]. Zirconium, which is represented by the symbol Zr and is in group 4B of the periodic table, is a bright, grayish-white colored element. The zircon mineral in the $ZrSiO_4$ composition and the Baddeleyite mineral in the ZrO_2 composition are the natural sources of the Zr element with economic value. Zirconium oxide (ZrO_2), which is obtained artificially from zirconium-silicate, whose name is the zircon mineral, is called zirconia in the market, just like alumina and magnesia. Other names for zirconium are 'zirconia or zirconium dioxide.

After the discovery of transformation toughening in 1975, ZrO_2 has been used extensively in science and technology [4]. As detailed in sections 2.2 and 2.3, this transformation of zirconia with three different polymorphs can be achieved more effectively by keeping the maximum tetragonal zirconia at room temperature. By adding metal oxide additives, it is possible to keep ZrO_2 in tetragonal and/or cubic phases at room temperature. Depending on the nature and amount of stabilizing oxide added, fully stabilized (FSZ, entirely cubic phase), partially stabilized (PSZ, mixture of tetragonal and cubic phases) and fully tetragonal polycrystalline zirconia (TZP, entirely tetragonal phase) can be obtained. Table 2.1 lists the properties of different zirconia products.

Zirconia is widely used in the manufacture of various dental implants due to its high hardness and density, excellent resistance to corrosion and different chemicals, and

various biocompatibility properties [5]. Thanks to these unique features, it is preferred not only for dental infrastructures, but also in other industries. Due to its toughness, mechanical resistance and thermal conductivity, it is used as an insulation material in the construction of automobile parts in the automotive industry, and in engine combustion chambers due to its high thermal expansion coefficient. Zirconium oxide is used in the production of cutting tools, wear-resistant machine parts, ceramic filters, fuel cells, oxygen sensors, turbine blades, piezoelectric and electrooptic circuits and capacitors. In addition to these, it is also used as a solid electrolyte, as a refractory material, as a ceramic coating material against oxidation and for thermal barrier purposes [4].

Table 2.1: Properties of different ZrO₂ products [6]

Properties	Material		
	Mg-PSZ	3Y-TZP	8Y-FSZ
Density (g/cm ³)	5.60	6.05	5.7
Flexural strength (20°C/800°C) (MPa)	545/354	1400/270	180/270
Compressive strength (MPa)	1700	2000	1500
Modulus of elasticity (GPa)	205	205	160
Poisson ratio	0.31	0.30	0.3
Hardness (HV _{0.3} , MPa)	1120	1350	700
Fracture Toughness (MPa.m ^{0.5})	6.0	5	3.5
Thermal expansion coefficient (x10 ⁻⁶ K ⁻¹)	10	10	11
Thermal conductivity (W/mK)	2.5	2	2.5
Thermal shock resistance (ΔT °C)	375	250	200
Specific heat capacity (J/kgK)	400	400	-

2.2 Crystal Structure of Zirconia

Zirconia has a polymorphic structure and has different crystal structures at different temperatures and pressures. The structure of pure zirconia from room temperature to 1000-1100°C is monoclinic and its density is 5.83 g/cm³. In this temperature interval, zirconia turns into tetragonal phase and its density increases (6.10 g/cm³). During cooling, a significant temperature hysteresis causes the transition temperature to shift to the range of 1000-900°C [2]. The tetragonal monoclinic phase transformation that occurs in the course of cooling is defined as diffusion free and martensitic transformation. During the transformation, large shear stress and a large increase (~4.5%) in volume occur. This phenomenon is also supported by the theoretical density values. At 2370°C, zirconia has a cubic phase structure and this phase structure continues until the melting temperature of zirconia. Fig. 2.1 and Table 2.2 illustrates the phase transitions of zirconia ceramic with density values and their characteristic crystallographic properties, respectively. Phase transformations that occur with an increase or decrease in temperature result in an increase or decrease in volume, and this causes stresses that lead to crack formation in the structure [7]. This situation creates problems in technological applications of ZrO₂. To overcome this problem, a partially or completely stabilized microstructure is needed.

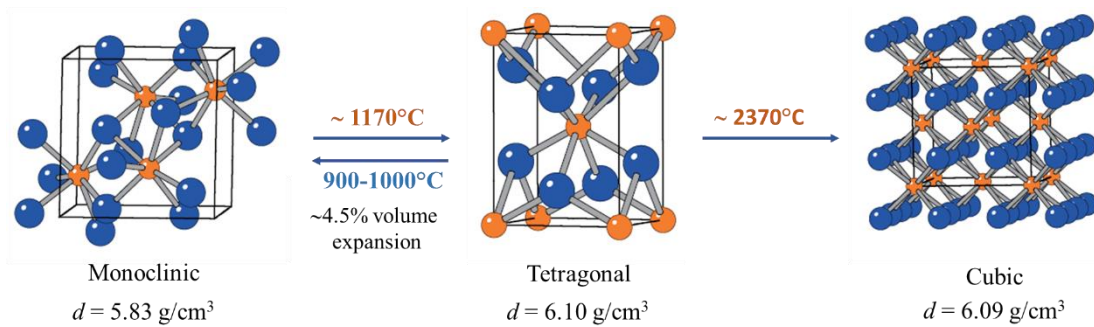


Figure 2.1: Crystal structures of zirconia polymorphs [6]

Table 2.2: Crystal structure of pure zirconia [8].

Phase	Space group	Space group number	Cation coordination number	Cell Parameters					
				a(Å)	b(Å)	c(Å)	α (°)	β (°)	γ (°)
Monoclinic	<i>P21/c</i>	14	7	5.1477	5.2030	5.3156	90.00	99.38	90.00
Tetragonal	<i>P42/nmc</i>	137	8	3.5948	3.5948	5.1824	90.00	90.00	90.00
Cubic	<i>Fm-3m</i>	225	8	5.1280	5.1280	5.1280	90.00	90.00	90.00

2.3 Stabilization of Zirconia

The existence of three structural forms of zirconia depending on temperature causes monoclinic zirconia to be unstable in terms of temperature-induced volume changes. This situation greatly limits the industrial applications of pure zirconia. However, as a result of studies on the fact that both hardness and toughness properties of zirconia can be increased by tetragonal-monoclinic phase change, it has been discovered that the desired phase can be stabilized at room temperature through various oxides. Stabilization is when zirconia forms a solid solution with ions of lower valence than itself. These low valence ions induce vacancies in the anion network, allowing to control the stress-induced t-m conversion and stop crack propagation efficiently. Until today, zirconia has been alloyed and stabilized with oxides such as CaO, MgO, Y₂O₃, CeO₂, Er₂O₃, Eu₂O₃, Gd₂O₃, Sc₂O₃, La₂O₃ and Yb₂O₃. In general, the most used stabilizers in biomaterial applications are CaO, MgO, Y₂O₃ and CeO₂ [2,9]; but only ZrO₂ and Y₂O₃ have ISO 13356 standard for surgical applications [10]. Moreover, the use of yttrium in partially stabilized zirconia particles has an important advantage because it can more effectively retain the tetragonal form at ambient temperatures [2].

By controlling the amount of stabilizing metal oxides, it is possible to obtain zirconia with different phases at room temperature. Partially stabilized zirconia (PSZ) and fully stabilized zirconia (FSZ) can be obtained from tetragonal polycrystals with increasing metal oxide additive ratios. The phases PSZ contains at room temperature are a mixture of monoclinic and cubic forms. FSZ is completely in cubic form. The diagram showing the relationship of ZrO₂ with metal oxide additions is given in Fig. 2.2.

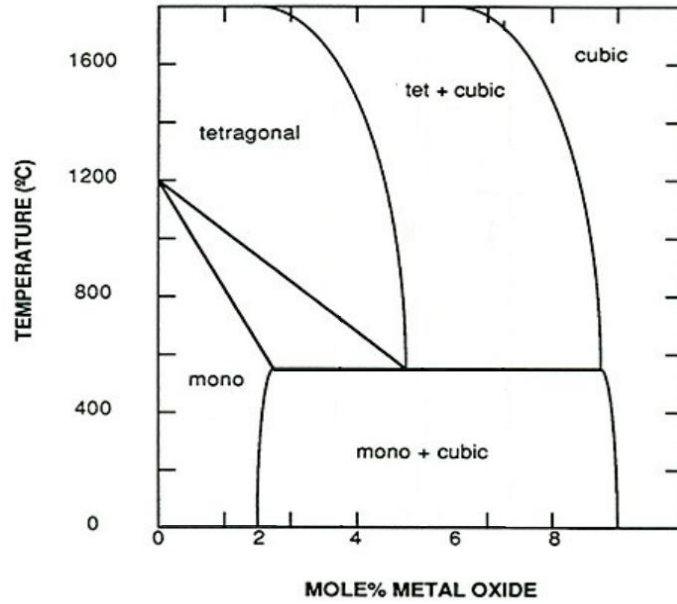


Figure 2.2: Schematic representation of zirconium oxide and metal oxide binary phase diagram [11].

2.4 Phase Diagram of ZrO_2 - Y_2O_3

The phase diagram of ZrO_2 - Y_2O_3 is given in Fig. 2.3. When the Y_2O_3 content is less than 1.5 mol%, the presence of only the monoclinic ZrO_2 phase is observed at low temperatures. At high temperatures, there is a wide tetragonal phase region. It is seen that when the Y_2O_3 content is more than 1.5 mol%, while the tetragonal and cubic ZrO_2 phase is preserved above about $1000^\circ C$, when the Y_2O_3 content is >9 mol%, a completely stabilized ZrO_2 solid solution in cubic form can be obtained.

In the stabilization process of zirconia with stabilizing oxides, it has been determined that the metastable tetragonal structure is approximately 98% by the sintering process in tetragonal zirconia polycrystals (TZP) where Y_2O_3 is used at a lower rate. It was observed that the mechanical strength increased with the increasing ratio of this tetragonal phase [1]. In Fig. 2.4, the graph showing the change in fracture toughness values, which is one of the important mechanical properties, is given according to the phase type that zirconia contains. Here, it is seen that tetragonal polycrystalline zirconia with a yttria content of 2-3% by mol reached the highest toughness values. At high yttria ratios, the phase structure of the zirconia ceramic changes, and its mechanical resistance decreases in terms of fracture toughness [13,14]. To obtain a

metastable tetragonal structure at room temperature, the particle size is as important as the yttria content. The critical particle size is 1 μm , depending on the Y_2O_3 concentration. While spontaneous t-m transformation takes place above this particle size, this transformation is inhibited in a too fine grained structure [14].

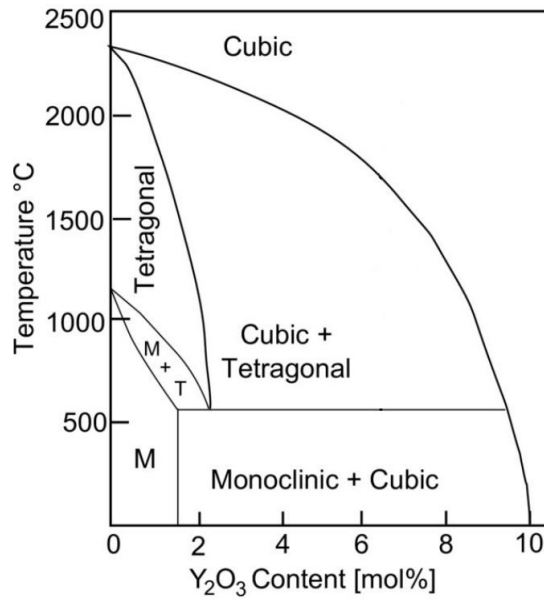


Figure 2.3: Phase diagram of the ZrO_2 - Y_2O_3 system [12].

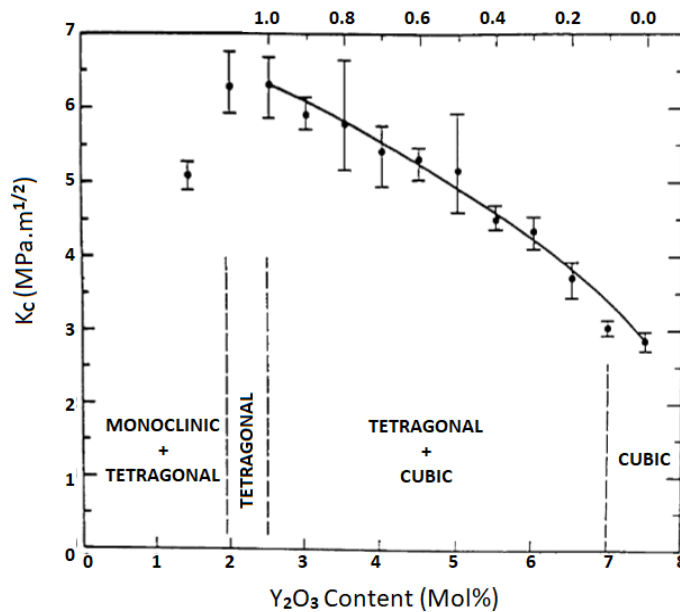


Figure 2.4: Phases and fracture toughness values of zirconia according to yttria content.

2.5 Transformation Toughness Mechanisms

As the zirconia ceramic cools down to temperatures lower than the sintering temperature, it transforms from tetragonal to monoclinic phase. Garvie et al. [15] stated that the increase in volume during this phase transformation in the stress area created by a crack in the ceramic body increases both the toughness and strength of zirconia ceramics. For this transformation, the tetragonal phase to survive at room temperature, the size of the zirconia particles must be smaller than a certain critical value. It is stated that this value is about $1\ \mu\text{m}$ [14,16]. The size of the zirconia particles is crucial to control the degree of stress-induced phase transition. If the grain size is much smaller than the critical size, the critical stress required to initiate toughness will be too high. Therefore, the toughening effect will be poor. As the grain size increases, the stress-induced phase change becomes easier and an increase in toughness occurs. The highest toughness values are achieved when all grains are slightly less than the critical grain [16].

A schematic representation of stress-induced transformation of zirconia grains is given in Fig. 2.5. In Fig. 2.6, the volumetric expansion and the magnitude of the shear stress occurring during the martensitic tetragonal-monoclinic transformation are illustrated. When crack formation occurs in the metastable tetragonal structure, a stress zone is formed in the impact area and end of the crack formed. This stress eliminates the main phase effect, which keeps the metastable structure under its influence. This time, the tensile stress acts on the structure and the tensile stress provides the transformation of the metastable tetragonal phase into the monoclinic phase.

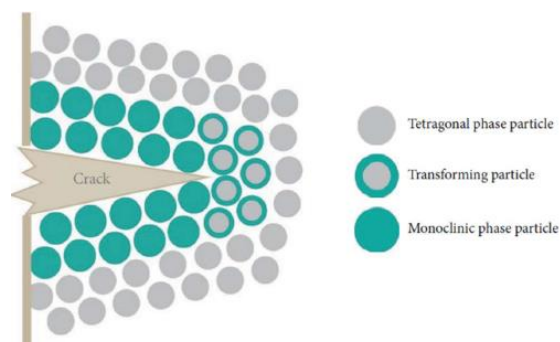


Figure 2.5: A schematic representation of the transformation of zirconia grains in the stress field of the crack by stress [17].

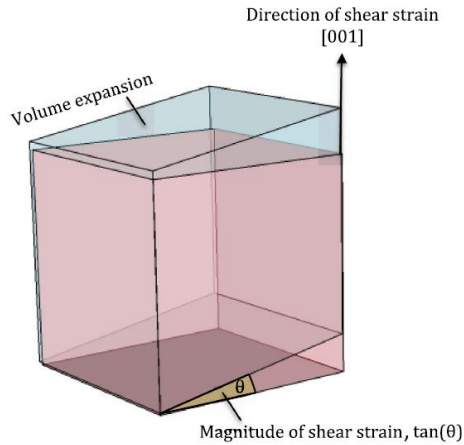


Figure 2.6: Schematic illustration of martensitic tetragonal to monoclinic transformation [18].

In the grinding-induced transformation, which is another toughening mechanism, a compressive stress can be created on the ceramic surface by surface grinding, which is a physical process. Grinding advances, the monoclinic transformation of metastable tetragonal grains and creates a print area approximately 10-100 μm deep of the surface. This compression stress significantly increases the mechanical resistance of the main phase in the body [1,19,20]. A schematic representation of the formation of compressive stress surface layers is shown in Fig. 2.7.

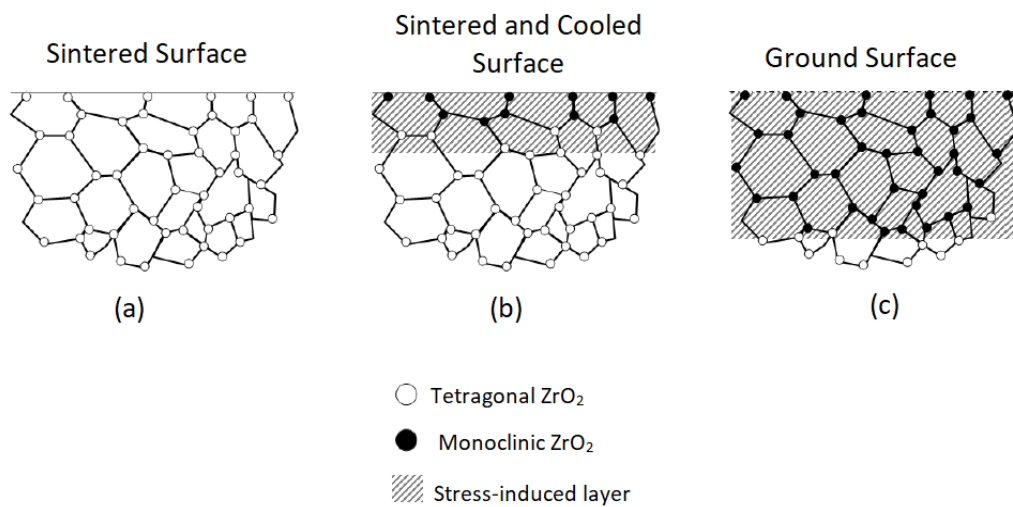


Figure 2.7: Schematic representation of grinding-induced phase transformation in surface layers [1,20].

2.6 Low Temperature Degradation (Aging)

Low temperature degradation (LTD) or aging is the state in which a tetragonal-monoclinic phase transformation occurs in the presence of water, steam, or liquids. This phenomenon occurs when water gradually penetrates the crystal structure, between temperatures of 200-400°C [17]. The phases of zirconia, which are repeatedly exposed to hot and humid environments, transform from tetragonal to monoclinic phases by moisture-induced. The transformation, which starts with the stress corrosion mechanism in the isolated grains on the surface first, causes surface deterioration, the formation of microcracks and ultimately a decrease in resistance in the long run [21,22]. Chevalier and Gremillard [23] have expressed the distribution of hydroxyl ions in the lattice in the ceramic body exposed to moisture in Fig. 2.8. They stated that the inward diffusion of moisture creates hydrostatic stress and changes the oxygen configuration around the Zr ions, both of which lead to the destabilization of the tetragonal phase. Tensile stresses are quite large at grain joints and edges and promote nucleation of the transformation. The nucleation and growth stage depend on microstructural properties such as porosity, residual stresses, and grain size. At this stage it is quite clear that both nucleation and growth will be highly process-related [22]. The transformation results in an increase in volume at the surface. The large shear stresses and displacements accompanying the transformation can create cracks along the grain boundaries. The cracks that form allow moisture to penetrate further into the material, and penetration continues as moisture ingress continues. Lawson [24], Miyazava et al. stated that they looked at the depth of penetration by polishing the transformed surface, and they found that the content of the monoclinic phase gradually decreased from the surface to the deep, and the depth of penetration increased with the aging time.

Aging tests are of great importance as microcracks that occur and grow due to thermal and mechanical effects can affect the mechanical performance and clinical success of zirconia-based ceramics. With the accelerated aging test, predictions can be made about the stability of bioceramics in the human body. According to the standard set by ISO 13356, the accelerated aging test should be performed in a steam autoclave at 134°C under 2 bar pressure for 5 hours [25]. ISO 13356 declared that the maximum amount of monoclinic phase should be 25% for clinical suitability after accelerated

aging testing. Although it is said that the 4-hour test period for this test applied in vitro corresponds to 40 years in vivo, Keuper et al. [26] stated that such definitions are doubtful based on the data they obtained after their in vivo aging experiments.

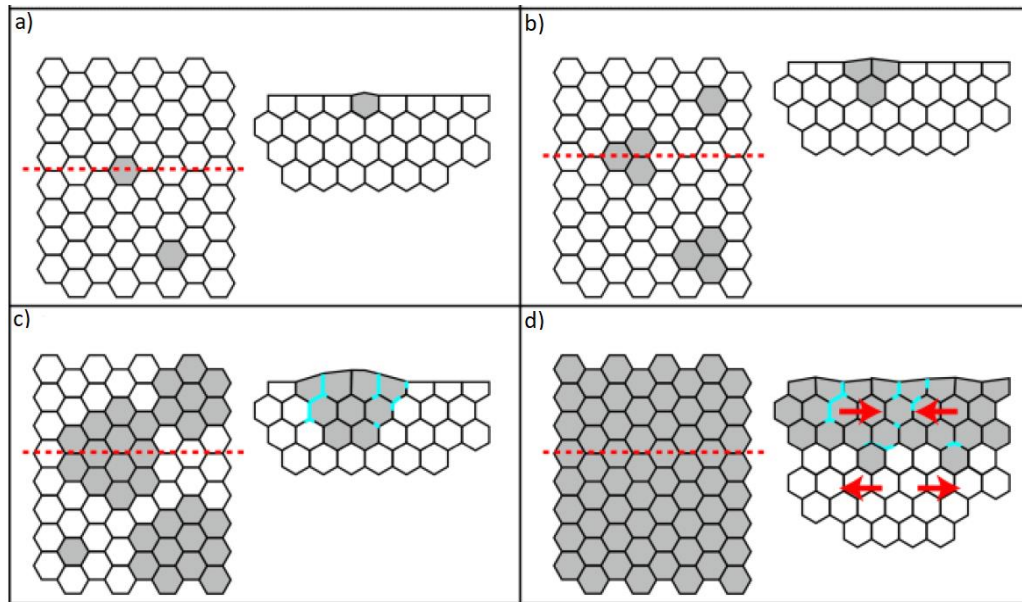


Figure 2.8: The steps of the low-temperature degradation process, (a)-(c) nucleation and growth of monoclinic phase in microscale, (c) the uplifts in the transformed regions occur and microcracks (in blue) are formed, (d) fully transformed surface, the transformation then proceeds to the bulk because water can penetrate through microcracks network.

2.7 Ceramic Powder Molding Methods

Ceramic materials can be formed by multiple methods such as slip casting, strip casting, extrusion and injection molding. Products with high density and strength required for advanced technology and dental applications can mostly be obtained by isostatic molding methods. The uniaxial dry pressing method is also often used in the first step of isostatic pressing.

2.7.1 Uniaxial Dry Pressing

This method is based on the principle of shaping the powders filled in the mold cavity by applying pressure in one direction or two directions. The ceramic raw material, which consists of blending the additives (binder) with the powder that will facilitate the shaping of the powders, is placed in the mold cavity and the desired product shape is given by applying pressure through the lower and/or upper pistons in hydraulic or mechanical presses. The schematic representation of the dry pressing method is given in Fig. 2.9. This method is a simple and easily applicable method and is generally used for mass production of small and simple parts.

The main reason why this method cannot be used for high-tech ceramic applications is that it cannot apply the molding pressure to the ceramic powder sample equally from all directions. The main reason why this method cannot be used for high-tech ceramic applications is that it cannot apply the molding pressure to the ceramic powder sample equally from all directions. This results in non-homogeneous firing shrinkage after sintering.

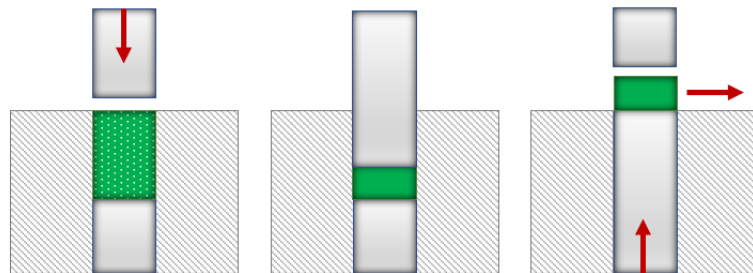


Figure 2.9: The schematic representation of the dry pressing method.

2.7.2 Isostatic Pressing

Isostatic pressing is a forming method that applies a uniform and equal force to the entire product, regardless of shape or size. This method removes many of the constraints that limit the geometry of unidirectionally clamped parts and offers the possibility to create product shapes to precise tolerances for many applications. The

process is used for a range of materials, including ceramics, metals, composites, plastics, and carbon. There are two basic methods of isostatic pressing. If isostatic pressing is applied at room temperature, it is called "Cold Isostatic Pressing (CIP)", if it is applied at high temperatures (2200°C), it is called "Hot Isostatic Pressing (HIP)".

Cold Isostatic Press (CIP), is a method used in shaping products of complex shape and quality that cannot be formed with dry press. This method is based on the principle of filling the ceramic raw material into the mold made of durable flexible rubber or synthetic material and shaping the material by ensuring that the hydraulic pressure is transferred homogeneously on the powder that will form the product. In order to transfer the pressure to the ceramic powder evenly from all directions, the medium to which the pressure is applied is chosen as water, oil or gas, thus providing hydrostatic press conditions. The cold isostatic press provides the possibility of a large volume end product with higher mechanical properties, as well as reducing the possibility of errors in the ceramic sample during pressing. It is possible to increase the density of the sample by increasing the CIP pressure [27].

Depending on the desired shape, it may be necessary to preform at a pressure of less than 30 MPa before production with this method. Products with higher density are obtained by applying high temperature sintering to the compacted part in CIP. In Fig. 2.10, the cold isostatic press and its application scheme are illustrated.

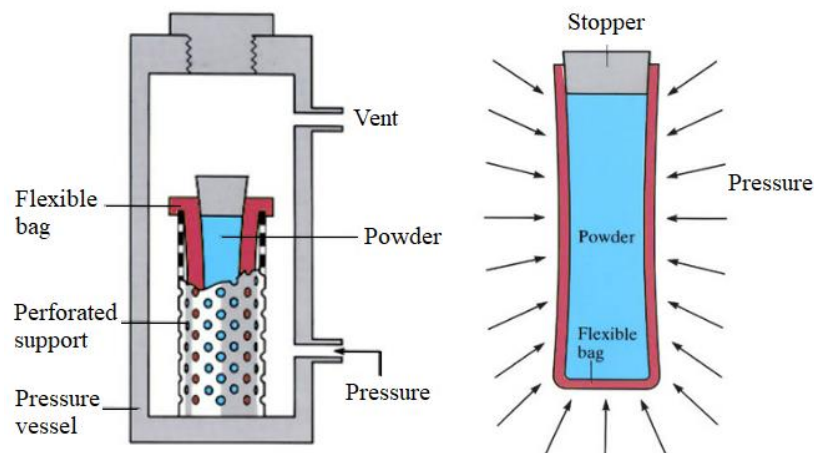


Figure 2.10: Cold isostatic press and application scheme [28].

Hot Isostatic Press (HIP), is technically similar to cold isostatic pressing (HIP). However, the main difference in hot pressing is that the hot mold assembly is located in a high temperature furnace. Temperature also affects the ceramic sample while pressure is applied. The pressing force is coaxial, and exposing the pressure vessel to heat ensures a full density (100% theoretical density) structure. The powder used in the HIP process does not have to be of high quality. Large pores are easily destroyed by the simultaneous effect of heat and pressure. High density is obtained at lower temperatures than is required in conventional pressureless sintering. By keeping the temperature low, excessive grain growth or secondary crystallization events do not occur. The disadvantage of this method is that the molds used at high temperatures are expensive and generally do not have a long life.

2.8 Sintering

Sintering can be defined as a thermally activated material transport phenomenon that causes the specific surface area of the shaped powders to decrease, the particle contacts points to enlarge and consequently the pore shape to change and the pore volume to decrease. Sintering is a heat treatment process that generally increases the strength and density and reduces the porosity by forming a bond between the particles in the part with the increase in temperature. The sintering mechanism is completely based on the transport of the material and the diffusion of atoms. In order to facilitate the transport of the material, the process takes place only at high temperature. In order for sintering to occur between two particles, it is necessary to exceed a certain temperature. This temperature range varies according to the type of material used. If the material to be sintered consists of a single type of metal or ceramic, it is called a one-component system, and if it consists of more than one material, it is called a multi-component system. While the sintering process is carried out at a temperature below the absolute melting temperature in single-component systems, it is generally performed above the melting temperature of the components with the lowest melting temperature in multi-component systems [29].

Ensuring full densification by sintering can be done in different ways. There are basically two types of sintering: solid phase sintering and liquid phase sintering. *Solid state sintering* is the process of forming bonds between particles by atomic transport

in the solid state at a temperature below the melting temperature. Considering the powders that are in contact with each other during sintering, since diffusion accelerates with high temperature, the powders interlock with each other by forming a neck in the first stage. In the middle stage of sintering there is further evolution of necks and pores. The pores spread to the grain boundaries and accumulate. In the last stage, with the formation of grain boundaries, the pores are gradually eliminated and densification is achieved. The stages and pore structures of ideal solid-state sintering is shown in Fig. 2.11.

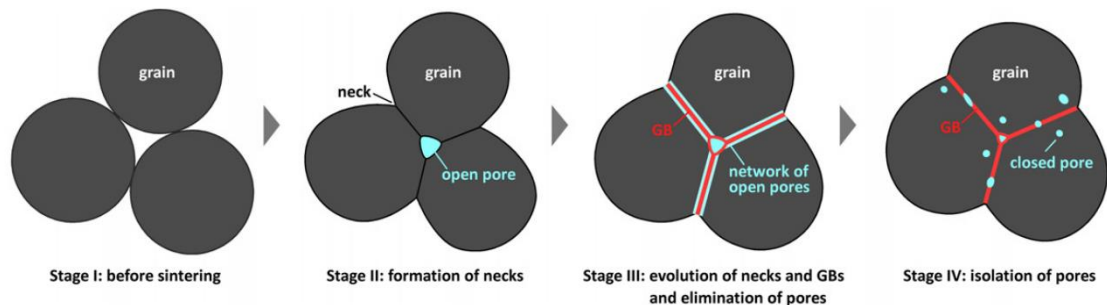


Figure 2.11: Schematic diagram of stages and pore structures of solid-state sintering [30].

Liquid phase sintering is a process for creating high-performance, multi-phase components. Melting points occur in the sintering of very different materials. A liquid phase coexists with a solid powder cluster at the sintering temperature. During sintering, the newly formed liquid penetrates between the solid grains, dissolves the sinter bonds and causes the grains to be rearranged. It increases bond formation between particles. The wetting angle of the liquid phase is an important parameter affecting sintering, and in this process, the wetting angle should be as small as possible. In liquid-phase sintering, it is possible to sinter ceramic powders at low temperature and in a short time. Fig. 2.12 shows the microstructure changes during liquid phase sintering [31,32].

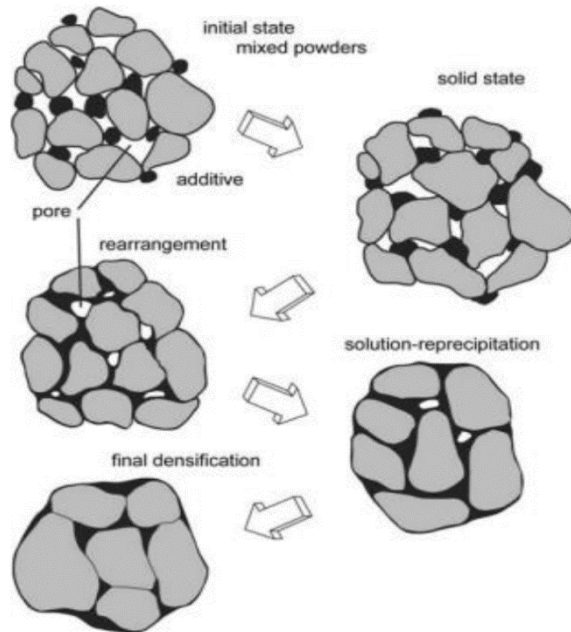


Figure 2.12: A schematic illustration of the microstructure changes during liquid phase sintering [32].

2.9 CAD/CAM System

Computer-aided design (CAD) and computer-aided manufacturing (CAM) system, which started to be used and developed in the field of dentistry in the 1980s, is one of the highly competent dental laboratory technologies. CAD/CAM systems are based on the acquisition of data using scanner tips, modeling of this data in a virtual environment, and the production of restorations with milling systems [33]. It basically consists of three main parts:

- i. **Scanner:** It is the data collecting component of the system. The data is obtained using a three-dimensional surface scanner that allows scanning directly through the mouth or over the model and digitized in accordance with the digital environment.
- ii. **Software:** It is the component that contains a computer program, in which the designs of the restorations to be obtained and intraoral planning can be made. The computer programs within the CAD/CAM systems have a library containing ready-made design models specific to each tooth. The system user

can use the existing designs in the software program or design their own three-dimensional virtual models.

- iii. **Hardware:** It is the component that includes the milling devices that can be controlled by the software system. The restoration designed in the software program is transferred to the production stage and is produced by etching from the blocks that are ready. All etching is carried out in the computer aided manufacturing unit.

The CAM process begins with selecting the appropriate block and placing it in the milling machine. Then, the grinding process starts in the designed model. A diamond coated disc with high velocity water spray is used to shape the ceramic restoration. The grinding process takes place at suitable angles with the rotation of the table on which the block is placed around its axis and the two-way movement of the diamond disc. Fig. 2.13 shows a sample pre-sintered block restored with CAD/CAM.

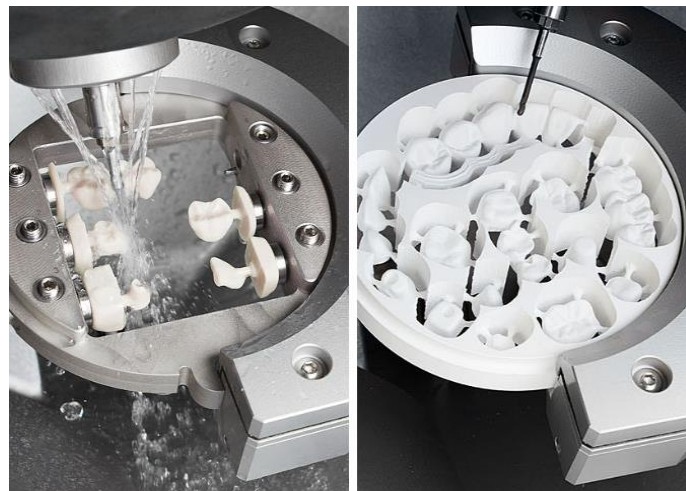


Figure 2.13: Restored pre-sintered block after CAD/CAM milling process.

CAD/CAM system is a practical application that saves time thanks to applications that can be done in a single session. Thanks to this method, with the elimination of traditional impression taking and plaster casting processes, the waiting time has been shortened and the possibility of errors that may arise from these processes has also decreased considerably. CAD/CAM systems, which have many advantages apart from the high initial cost, also provide economic gains thanks to the reduction in the number

of sessions. In addition, it enables the production of restorations with better edge compatibility, surface quality, mechanical resistance and aesthetic properties. Taking digital impressions with an intraoral camera offers a more comfortable session for both patients and physicians. In addition to these, the database in which the data is stored allows it to be reproduced quickly and easily in adverse situations such as the restoration of fracture or loss [34–36].

2.10 Recycling of Dental Zirconia Ceramics

In addition to the advantages of the widespread use of CAD/CAM systems in dentistry mentioned in Chapter 2.8, it is a significant disadvantage of this method that it generates a tremendous amount of waste, especially after the processing of zirconia, one of the most expensive dental ceramics today. A dental zirconia block loses approximately 30% of material after it has been processed. Considering that each block can always have unprocessed parts, it has been stated that the amount of waste produced can reach up to 80% of the initial mass [37]. From an environmental and economic point of view, the recycling of this waste and its reuse as a high value-added material will have obvious benefits. With this motivation, some studies have been carried out to evaluate the recycling possibility of the waste generated after the CAD/CAM processing of dental zirconia blocks. Sriboonpeng et al., [38] to investigate the production of ceramic bodies with properties comparable to commercially used pre-sintered zirconia blocks, succeeded in recycling waste zirconia blocks at nano-size by vibro-milling method and determined the optimum parameters with the help of particle size, phase analysis, and morphological properties. In their later studies [39], they sintered the recycled zirconia at various temperatures (from 1100°C to 1250°C), and then evaluated its physical and mechanical properties. When the results were compared with the control group, they stated that their approach was a promising strategy to recycle CAD/CAM zirconia wastes.

Abed and Al-Manaf [40] recycled the pre-sintered waste dental zirconia blocks by grinding, and then investigated the recyclability and machinability of the blocks at different uniaxial compression pressures (75, 100, and 145 MPa) and different pre-sintering temperatures (950°C and 1100°C). They concluded that blocks pre-sintered at 950°C can be reworked with CAD/CAM, as they show similar results to commercial

blocks. Silva et al. [41] conducted a similar study and used different printing methods. Recycled zirconia blocks were pressed both uniaxially (50 MPa) and isostatically (200 MPa) and then sintered at 1500°C. They stated that ceramics produced by isostatic pressing have higher density and mechanical properties in accordance with commercial samples, therefore it is possible to use recycled zirconia powder as raw material in the same original process.

Kim et al [42] evaluated the possibility of recycling the remaining parts of the zirconia block after CAD/CAM using the slip casting process. They examined the physical and mechanical properties of the recycled zirconia powder after pre-sintering at 1000°C and sintering at various temperatures. In this study, in which 1500°C temperature was accepted as optimum, it was stated that it is possible to use cast zirconia samples with 200-300 nm grain size, 0% apparent porosity and 680 MPa flexural strength in ceramic prostheses.

There are studies in the literature for the recycling of waste zirconia obtained after the CAD/CAM processing process and its usability in different areas. Cossu et al. [43] aimed to develop Al₂O₃-ZrO₂ ceramic composites using recycled ZrO₂(Y₂O₃) source from dental blocks. When the mechanical and physical properties of the produced ceramic composites were evaluated, they concluded that the waste zirconia additive was effective in the development of the composite. Erdoğan and Karslıoğlu [44] produced PMMA reinforced with recycled zirconia powder from waste blocks to increase mechanical strength in PMMA-based temporary restorations. They observed the positive effects of YSZ contribution up to 60% in mechanical terms. Thus, they stated that residual yttria stabilized zirconia powder would increase the chance of use and PMMA would have a safer use.

Gouveia et al. [37], by adding 5%, 10% and 50% recycled zirconia powder from waste blocks to yttria-added commercial zirconia powder, conducted a detailed study to determine the potential uses of recycled dental zirconia. This study includes the physical properties and chemical composition of the waste powder, elastic modulus, color analysis, microstructure and mechanical properties for the prepared recycled mixtures. According to the results of the analysis, they stated that the waste zirconia powder, which does not contain contamination and monoclinic phase, offers extremely good properties to be used as zirconia sandblasting for prostheses and as a raw material

for the refractory and pigment industry. They declared that all mixtures can be used as jewelry and pigment in industries with a color difference requirement of $\Delta E^* < 1$, and that only 5% waste zirconia additive sample provides sufficiency for dental applications.

To investigate their effective reuse in dental prostheses, Ding et al. [45] aimed to investigate an easier and cleaner method of recycling residues from dental CAD/CAM zirconia blocks. In their work, they first cleaned the waste zirconia powders, then ground it in nitric acid and started the production process. They subjected the samples they produced to seven different pre-sintering temperatures (800, 850, 900, 950, 1000, 1050, and 1100°C) and sintered them for 2h at 1450°C according to the manufacturer's recommendation. In addition to physical properties such as phase analysis, chemical composition, surface morphology, density, machinability, shrinkage rate of the samples obtained, mechanical properties such as hardness and flexural strength were investigated, and the results were compared with the control group. Considering the mechanical behavior of the samples, it was observed that the mechanical properties decreased with the increase of abnormal grain growth in the samples pre-sintered above 1000°C, therefore it was concluded that the ideal pre-sintering temperature was 950-1000°C. All experimental results showed that the samples obtained with the recycled powder from the waste blocks exhibited very similar physical and chemical properties with the control group. However, Ding et al. stated that further studies are needed to examine clinical trials of restorations made from recycled products.

As a recent and current study, Cordeiro et al. [46] applied two experimental protocols (de-agglomerated and agglomerated) to dental zirconia obtained from blocks, applying the effect of GM (grinding medium mass)/M (zirconia waste powder mass), (13 and 22) at different grinding times (30, 60, 90, and 180 min.) studied. They characterized the samples they sintered at 1300°C, 1400°C and 1500°C and compared the results with commercial zirconia. As a result, they stated that the de-agglomeration process is an important process to achieve the best physical and mechanical properties in the recovery of zirconia. They found that the samples with a GM/M of 13 and milled for 90 minutes had the lowest particle size and phase transformation. They observed that the de-deglomerated samples sintered at 1500°C had density and hardness values that gave the closest results to commercial powder. Finally, the de-agglomerated samples

sintered at 1400°C have reached the highest bending strength. This value was 342 ± 66.7 MPa, which was quite low compared to commercial zirconia (680.5 ± 96.0 MPa). Therefore, Cordeiro et al. stated that dental zirconia recycled from waste blocks is likely to be used as an alternative dental material to porcelain or lithium disilicate ceramics in low to medium stress conditions such as anterior crowns. In addition, they emphasized that more studies are needed for the application of zirconia waste powder as a dental material despite its high potential.

Chapter 3

Experimental Procedure

3.1 Materials

Within the scope of this thesis, Shenzhen Upcera Super Translucent pre-sintered zirconia block wastes (Fig. 3.1) stabilized with 3 mol.% (wt. 5%) Ytria (Y_2O_3) and processed in CAD/CAM, which formed the basis of the study, were obtained from a local dental laboratory. The chemical composition and physical properties of zirconia blocks with high purity (99%) and theoretical density ($>6 \text{ g/cm}^3$) provided by the manufacturer are presented in Table 3.1.



Figure 3.1: CAD/CAM machined pre-sintered zirconia block

Table 3.1: Chemical composition and some physical properties of Upcera powder

UPCERA	
Chemical Composition (wt.%)	
Zr ₂ O + Hf ₂ O + Y ₂ O ₃	≥ 99
Y ₂ O ₃	4.5-6.0
Al ₂ O ₃	0.1
Other Oxides	≤ 0.5
Physical Properties	
Density	0.6 ± 0.01 g/cm ³
Flexural Strength	>1200 MPa
Chemical Solubility	100 µg.cm ⁻²
Linear Thermal Expansion Coefficient	10.5 ± 0.5 x 10 ⁻⁶ .K ⁻¹

*Source: Shenzhen Upcera Dental Technology Co., Ltd

The commercial powder to which the recycled powder will be added was 3-mol percentage (mol %) yttria (Y₂O₃) coded TZ-3YS-E stabilized zirconia produced by Tosoh Cooperation (Lot S304599P, Japan). Here, Y symbolizes yttria, and S and E also present grade names. Since S-grade zirconia has a smaller surface area, it contributes to the flow in molding methods and is substantially recommended for production using a mechanical press or CIP. E-grade zirconia has also easy sintering properties. The actual particle size of the powder is declared to be 40 nm. Physical properties and chemical composition in weight percentage (wt. %) of the powder are listed in Table 3.2.

Polyvinyl alcohol (PVA) produced by Sigma Aldrich (Lot number: SLBF3965V) was preferred as the binder that contributes to the adherence of the powders. The average molar weight of PVA, which is 87-90% hydrolyzed, is in the range of 30,000-70,000.

Table 3.2: Chemical composition and some physical properties of Tosoh TZ-3YS-E powder [48]

TOSOH TZ-3YS-E	
Chemical Composition (wt.%)	
Y ₂ O ₃	5.2 ± 0.5
Hf ₂ O	< 5.0
Al ₂ O ₃	0.1 – 0.4
SiO ₂	≤ 0.02
Fe ₂ O ₃	≤ 0.01
Na ₂ O	≤ 0.04
Physical Properties	
Density	> 0.6 g/cm ³
Flexural Strength	>1200 MPa
Fracture Toughness	5 MPa.m ^{0.5}
Hardness (HV10)	1250

*Source: Tosoh Europe B.V.

3.2 Method

3.2.1 Production of Samples

The flow chart of the processes applied from raw materials to final products within the scope of this study is given in Fig. 3.2. Waste zirconia blocks, which were collected in sufficient quantity from a local dental laboratory, were crushed to a size of approximately 1.5-2 cm before recycling operations could be initiated. Then, the crushed blocks were pulverized for 10 minutes at 1000 rpm on a vibrating disc mill (RS200, Retsch, Germany), which is a very fast and successful method of grinding. Afterward obtained powders were sieved with the help of a sieve shaker (AS 200, Retsch, Germany) through 45 μm screen.

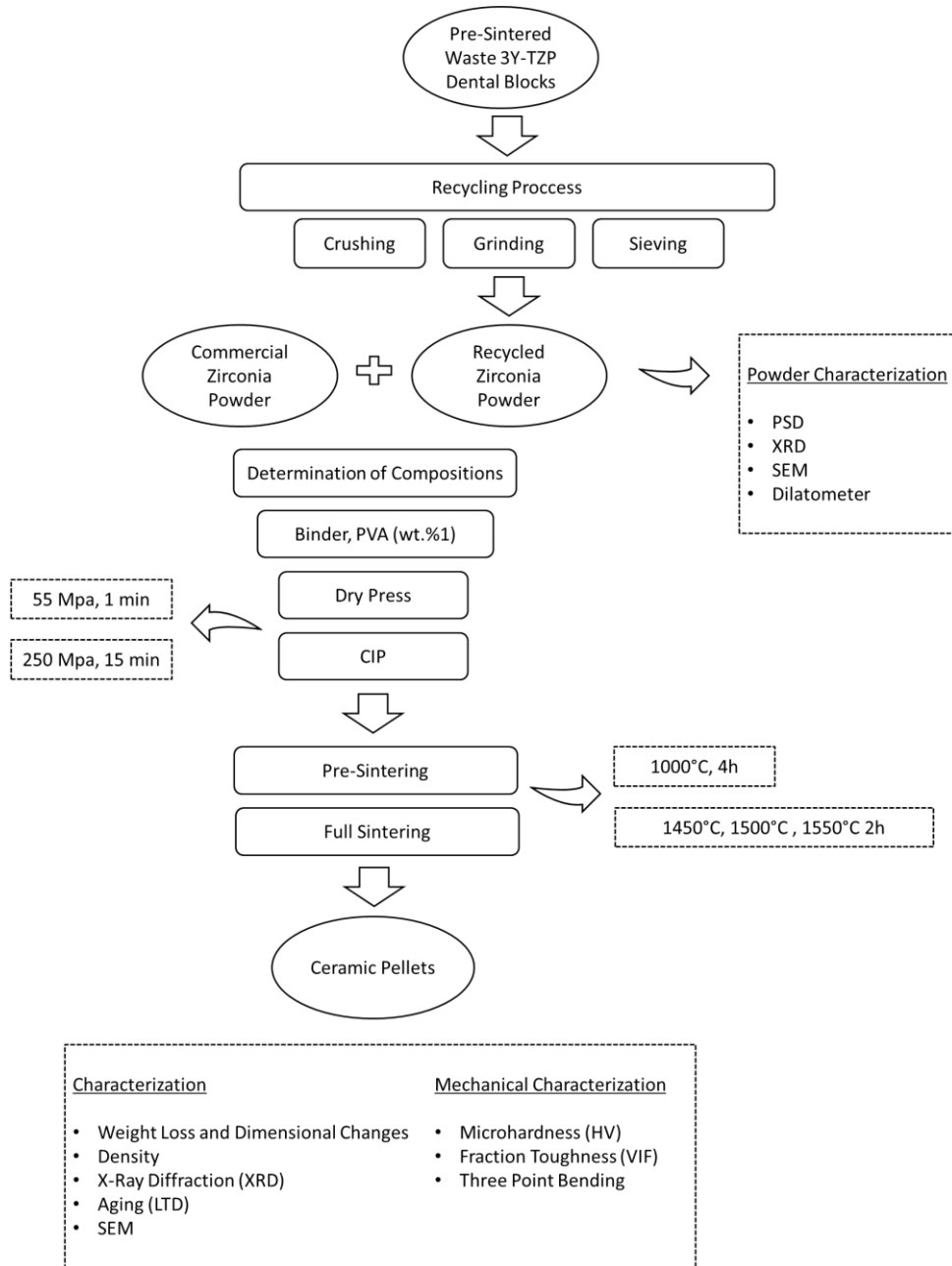


Figure 3.2: Flow chart of the production steps of the samples

Raw material characterization was performed on powders reduced to suitable size. The recycled powder was added to the commercial powder at the rates specified in Table 3.3 and mixed in a cylindrical mill at 200 rpm for 2 hours in order to ensure homogeneous distribution of the powders. Samples were named with regard to % waste zirconia content. In sample names R stands for recycled powder, YSZ means yttria stabilized zirconia. The commercial powder, which had no waste powder additions at all, was denoted with 'COM'.

Table 3.3: Sample names and waste zirconia contents

Sample Code	Waste zirconia additive amount (%)	Commercial zirconia (%)
COM	0	100
3R-YSZ	3	97
5R-YSZ	5	95
10R-YSZ	10	90
15R-YSZ	15	85
30R-YSZ	30	70
50R-YSZ	50	50
100R-YSZ	100	0

Current study was performed in three sets of experiments due to the sintering temperatures (1450°C, 1500°C, and 1550°C). There are 8 samples in each set. The numbers 145, 150 and 155 next to the sample code in the following sections will represent the sintering temperatures.

Considering the yield obtained from the binder trials in the literature and the small powder size [4], the samples were mixed homogeneously with only 1% PVA by weight before being brought into pellet form. 3 g of powder prepared for pressing at all mixing ratios was compressed by a uniaxial hydraulic press in a cylindrical die made of stainless steel with a diameter of 15 mm by applying an external pressure of 55 MPa for 60 seconds. The dry pressed samples are shown in Fig. 3.3. To increase the density of the compact, the samples were then applied cold isostatic press (CIP) at 250 MPa pressure. Before applying pressure, all samples were carefully placed in a special vacuum bag to prevent contact with the liquid and vacuumed with the help of a vacuum packaging machine (VolvacW42, Hannover, Germany). The vacuumed samples were then placed in a pressing chamber filled with a water-boron oil mixture. Here, all samples were exposed to isostatic pressure for 15 minutes. After the CIP process, weight and dimensional measurements of all samples were performed.



Figure 3.3: Dry pressed samples

3.2.2 Pre-sintering and Sintering Processes

Pre-sintering is a pre-process that is carried out to remove the binder in the zirconia that has been brought into block form and to make it easy to process in CAD/CAM before sintering. Protherm, PLF 160/15 model high temperature furnace was used for sintering processes. The pre-sintering and sintering steps applied for this study are illustrated in Fig. 3.4.

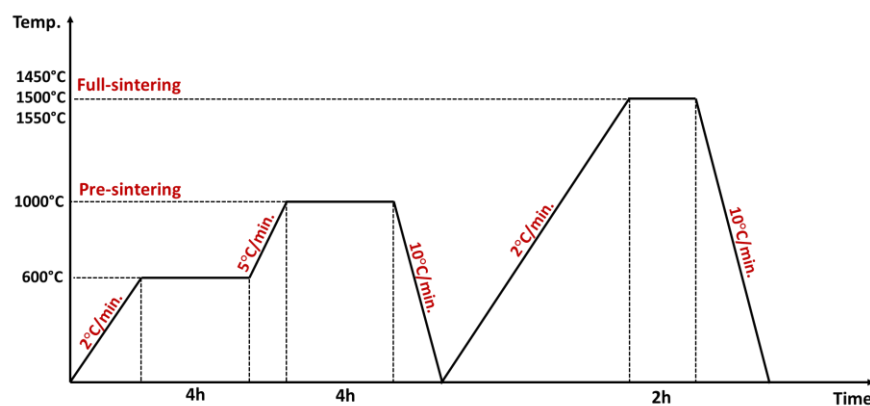


Figure 3.4: Pre-sintering and full-sintering schedule

Pre-sintering was carried out in two steps. In the first step, the samples were primarily up to 600°C with a heating rate of 2°C/min. and kept at this temperature for 4 hours. Then it was up to 1000°C at a heating rate of 5°C/min, and after being kept there for 4

hours, it was cooled to room temperature with a cooling rate of 10°C/min. In the full-sintering stage, the heating rate was 2°C/min from room temperatures up to determined temperatures (1450°C, 1500°C, and 1550°C). After the sintering time of 2 hours was completed, the samples were cooled to ambient temperatures with cooling rates 10°C/min.

3.3 Characterization of Samples

3.3.1 Particle Size Analysis

The grain size distributions of purchased commercial powder (TOSOH) and recycled zirconia powder (UPCERA) raw materials from the processed block were determined using the Malvern Mastersizer 2000 laser diffraction particle size instrument. With this instrument, particle size distribution analysis of powders with dimensions between 0.02 µm and 2000 µm can be performed.

The ground zirconia powders were finely ground for a while with the help of an agate mortar in order to remove possible agglomerations. Then, each powder was mixed by adding some amount into a beaker filled with approximately 10 ml of distilled water and left in an ultrasonic bath (Sonorex Super, RK106) for 5 minutes. At this stage, the sedimentation of the powders to the bottom of the beaker was prevented and the powders were suspended. Analysis was carried out by dropping a few drops from the suspension in the beaker into the measuring chamber of the grain size analyzer. Dust particles floating in the aqueous medium are exposed to laser beams and the beams are scattered by diffraction at different angles depending on the size of the particles. The scattered rays are collected on a converging lens and focused on the detector. The beams reflected on the detector are digitized by a transducer and the grain size and percentage are calculated by means of a computer program.

3.3.2 Differential Thermal Analysis

The thermal behaviors of polyvinyl alcohol (PVA) were investigated under nitrogen (N₂) flowing with the help of the Perkin Elmer STA 8000 appliance. Thermal data were analyzed using a software program supplied with the instruments. In this

experiment, the heating regime was determined as 10°C/min from 25°C to 1000°C under a nitrogen atmosphere.

3.3.3 Weight Loss and Dimensional Change Measurements

For the purpose of calculate the dimensional changes and weight losses of the dry pressed samples after cold isostatic pressing, pre-sinter and sinter processes, diameter, height, and weight measurements of the samples were carried out after each process.

For dimensional changes, the diameters and heights of the selected dry pressed samples were measured by precision digital caliper immediately after processing. The two digits after the comma were taken into account when recording the mathematical data. After the cold isostatic press, pre-sintering and sintering processes, the diameters and heights of all selected samples were measured and recorded with the same precision. For each sintering temperature, 5 samples from each composition were used in this process, and all results were averaged by performing at least 3 measurements from each sample. The dimensional volumes of the samples were also calculated with the obtained data.

Diameter change, height change and volume change before and after the procedure were calculated as percent. Weight measurements of selected samples were performed using a Denver, SI-234 brand precision balance. In the measurements made before and after the process, the percent weight loss in course of the process was computed.

3.3.4 Optical Dilatometer

Optical dilatometry analysis was performed on the prepared powder mixtures in order to obtain a prediction about their sintering behavior and to examine their behavior at high temperatures. For this, Misura brand Optical Dilatometer and Heat Microscope (Misura 3 ODHT) device was utilized. Samples containing different proportions of waste zirconia powder were printed in small square prism-shaped bars, approximately 15 mm high and 5x5 mm thick, and placed in the furnace area of the device. By applying a standard heat treatment regime to the samples, 10°C/min. The heating rate was increased to 1300°C rapidly and the device was cooled at this temperature, which is the maximum capacity, without waiting.

The optical dilatometer device can measure the dimensional change of the sample such as shrinkage and expansion during the heating process, without applying any force on the sample through an optical system. With the help of a heat microscope, the dimensional changes of the sample are recorded and after the completion of the experiment, various curves are obtained by using the computer software of the device to exhibit the sintering behavior of the sample. By means of these curves, it is possible to examine the behavior of the sample during sintering, to estimate the approximate sintering temperature and to determine the transformation temperatures.

3.3.5 Density Measurements

After the pre-sintering and sintering processes, density measurement was carried out on the samples selected from all compositions in each set, based on the Archimedes principle. 3 different samples were selected from each composition and the averages were taken by weighing 3 times. The density results of the produced samples were compared with the samples obtained from the original block.

For density measurement, primarily selected samples were weighed dry (D). Each sample was then placed in a beaker of distilled water and boiled on a heat plate for 2 hours. It was then allowed to cool to room temperature. In the Archimedes kit shown in Fig. 3.5, the suspended weight (S) of the sample was calculated by placing it on a hanger in a beaker full of distilled water. Afterward this process, each specimen was blotted lightly with a moistened smooth napkin to remove all drops of water from the surface and was determined the saturated weight (W) by weighting again.

The volumes, bulk densities, apparent specific gravity and apparent porosity of the samples were calculated using Equation (3.1), Equation (3.2), Equation (3.3) ve Equation (3.4) respectively.

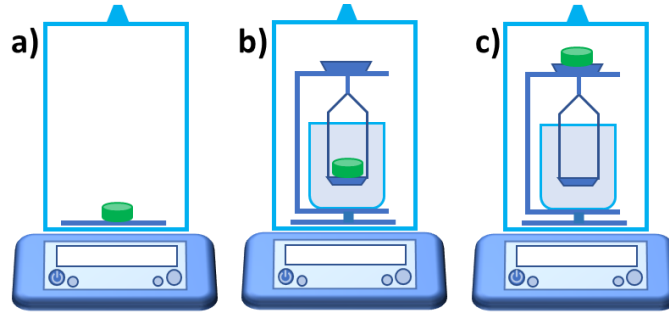


Figure 3.5: Schematic representation of (a) dry weight, D , (b) suspended weight, S , and (c) saturated weight, W measurements according to Archimedes' principle

$$\text{Volume, } V = W - S \quad (3.1)$$

$$\text{Bulk Density, } B = D/V \quad (3.2)$$

$$\text{Apparent Specific Gravity, } T = D/(D - S) \quad (3.3)$$

$$\text{Apparent Porosity, } P, \% = [(W - D)/S] \times 100 \quad (3.4)$$

3.3.6 Accelerated Aging Test

To investigate the stability of the tetragonal phase against hydrothermal aging, the accelerated aging test was applied to the sintered samples. The International Organization for Standardization (ISO) 13356 Implants for Surgery has established a standard procedure for accelerating the aging of medical zirconia [3], and according to this standard, the specimens placed in a suitable autoclave should be exposed to steam for 5 hours at $134 \pm 2^\circ\text{C}$ under a pressure of 0.2 MPa [4]. Since the aging procedure is based on from the tetragonal to monoclinic phase transformation of dental zirconia at moderate temperatures (below 400°C), this process is also denominated low-temperature degradation (LTD) [5].

Parr 4842 series hydrothermal device was used for the aging tendencies of the samples sintered at 1450°C , 1500°C and 1550°C , and 2 bar water vapor pressure was applied to all samples at 134°C for 5,10 and 15 hours in accordance with the protocol

determined by ISO 13356:2008. The aging tendency of the samples was determined using Equation (3.5) depending on the phase changes observed in the XRD analysis results.

3.3.7 X-Ray Diffraction (XRD) Analysis

Crystalline phases of the recycled powders, and samples produced from the bodies prepared within the scope of the studies and subjected to sintering heat treatment at different temperatures were analyzed at room temperature using an X-ray diffractometer (XRD, Bruker D2 Phaser). The X-ray diffraction data were recorded by using Cu K α radiation (1.5406 Å). The intensity data were collected over a 2 θ range of 5°-90° with scanning rate of 0.176 and during 900 sec. ICDD database was utilized for identification of tetragonal and monoclinic phases of zirconia.

The effect of LTD test on phase transformations was estimated by the intensities of the most intense X-ray reflections for the tetragonal and monoclinic phases, using the method proposed by Garvie et al. and Toroya et al. [47,48]. The amount of transformed zirconia phase from tetragonal to monoclinic was calculated employing following equation.

$$X_m = \frac{I_m(\bar{1}11) + I_m(111)}{I_m(\bar{1}11) + I_t(101) + I_m(111)} \quad (3.5)$$

Here, X_m is the monoclinic phase fraction, the subscripts m and t refer to the monoclinic and tetragonal phases, respectively and $I_{(hkl)}$ denotes the integrated intensity of the diffraction line indicated by its Miller indices. V_m is volume fraction of monoclinic ZrO₂ and 1.311 is the correlation factor.

3.3.8 Scanning Electron Microscopy (SEM)

The morphology of the sintered samples, and the size, and shape of the grains were investigated with a Phillips brand XL-30 SFEG model scanning electron microscope. Before microstructural analysis, first of all, the surface of the samples was made suitable for analysis. For this purpose, the samples to be examined were subjected to a

series of surface preparation processes. Sintered samples in pellet form were cut with a precision cutter and placed in a plastic mold to ensure that these pieces remain in a fixed position and are easily held during polishing. Afterward, LED UV polyester resin stabilized in styrene was poured into the mold. The photocatalyzed resin was held under UV light for 10 minutes and the resin was allowed to cure. The surface of the samples embedded in the resin was subjected to sanding and polishing processes to make it suitable for microstructure analysis. To this end, the surface was abraded with a series of SiC abrasives ranging from coarse to fine, and then the polishing process was completed by employing diamond paste. A thermal etching process was applied in order to make the grain boundaries clear on the polished surfaces. This process was carried out for the samples sintered at different temperatures by keeping them at 150°C below the sintering temperature for 45 minutes. Afterward, the surfaces of the thermal etched samples were covered with a gold film to provide conductivity so that they can be examined in SEM. Based on the obtained micrographs, the average grain size of each sample was calculated by digital image analysis of the Image J program using the linear intersection method defined in EN 623-3 Method A [49].

3.3.9 Measuring Mechanical Properties

3.3.9.1 Microhardness

The microhardness measurement of the sintered samples, whose surfaces were precisely polished, were made using the Vickers diamond pyramid tip on the Sinowon® brand HV-1000D model Microhardness device. Microhardness measurements were performed to each sample from 8 different regions under 1 kgf load for 15 seconds. The average hardness value was determined by taking the average of the results obtained. Microhardness measurements were carried out in 8 different regions under 1 kgf load for 15 seconds. The shapes illustrated in Fig. 3.6 were attained on the sample surface, and the microhardness values were computed using Equation 3.6. The average microhardness value of each sample was determined by taking the average of the results.

$$H_v = 1.8544 \frac{P}{d^2} \quad (3.6)$$

Where, the H_v is Vickers hardness, the P is load (kgf), and d is the sum of the diagonal lengths (mm).

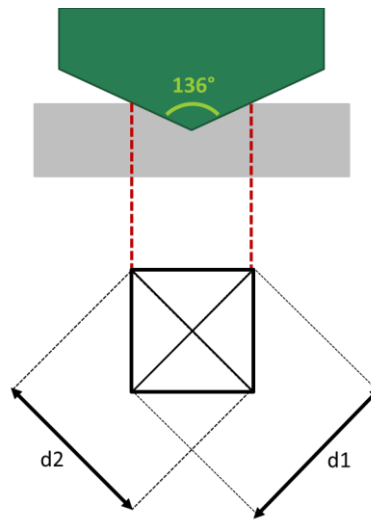


Figure 3.6: Schematic representation of the Vickers hardness measurement method and the shape of the trace

3.3.9.2 Indentation fracture toughness

The indentation fracture (IF) method is frequently applied in dentistry to determine a fracture toughness value because the test method is easy and simple. In the IF method, the fracture toughness value is calculated based on the lengths of the marks and cracks created by notching a Vickers indentation in the polished specimen against the test specimens [50]. In this study, Instron (Wolpert Testor, 2100 model) brand hardness measuring device with pyramidal diamond indenter was used to calculate the fracture toughness values. The samples were cracked by keeping them under 10 kgf load for 10 seconds, then the crack lengths obtained were measured with the help of an optical microscope. This process was carried out in 5 different regions for the same sample. The fracture toughness values of the samples were calculated using the Equation 3.7

suggested by Antis et al. [51]. The average fracture toughness values were determined by taking the average of the results.

$$K_{1c} = 0.016 \left[\frac{E}{H_v} \right]^{1/2} \frac{P}{c^{3/2}} \quad (3.7)$$

Where; K_{1c} (MPa. \sqrt{m}) is fracture toughness, P (N) is load, distance from crack tip to center of trace is c (m), H_v denotes hardness (MPa), and E denotes elastic modulus and was accepted as 210 GPa in this study. A schematic representation of the Vickers indentation used to determine fracture toughness values is shown in Fig. 3.7.

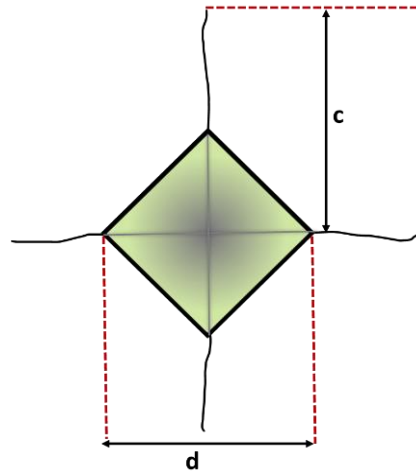


Figure 3.7: A schematic representation of Vickers indentation and c , crack length

3.3.9.3 Three-point Bending Test

For the three-point bending strength test of the selected samples, powder mixtures prepared from the selected compositions were pressed in the form of a rectangular prism in a stainless-steel die with 5 mm x 5 mm x 70 mm. The bending test specimens produced were first exposed to cold isostatic pressing (CIP) under 250 MPa for 15 minutes, following the production methods standardized in this thesis. Subsequently, the binder removal and sintering steps detailed in Fig. 3.4 were applied.

The samples ready for testing were tested in the experimental setup of Instron, Model 4202 device according to ISO 6872-2015 method. The schematic representation of the experimental setup is given in Fig. 3.8. The outer opening was determined as 40 mm and the three-point bending test was performed by applying the varying load at a speed of 0.5 mm/min.

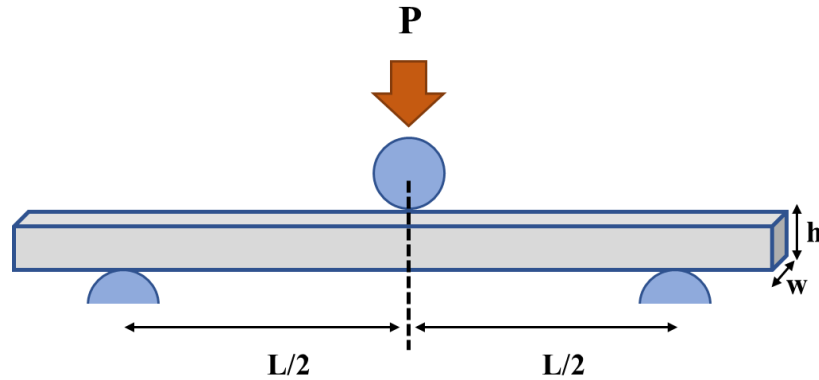


Figure 3.8: Schematic representation of the three-point bending test setup

The maximum load at the time of fracture of the samples was accepted as the breaking load and the bending strength of the samples was calculated using these load values. The formula used to calculate the bending strength values is given in Equation 3.9. These calculations were carried out during the measurement by the software in the device operating under computer control. The average of the measurement results was recorded as the bending strength value.

$$\sigma = \left[\frac{3PL}{2wh^2} \right] \quad (3.9)$$

In this equation; σ = bending strength (MPa), P= maximum applied load (N), L= distance between supports (mm), h= thickness of sample (mm), w= width of sample (mm).

Chapter 4

Results and Discussion

4.1 Raw Material Characterization Results

4.1.1 Particle Size Distribution Results

Particle size distribution analysis was applied to commercial zirconia powder (COM) and recycled zirconia powder (R-YSZ) used as raw materials before production processes. Fig. 4.1 shows the particle size distribution graph of recycled zirconia powder. As the chart shows, the average particle size (D50) of recycled zirconia powder is below 12 microns, while 90 percent (D90) is below 30 microns. Fig. 4.2 illustrate the particle size distribution of commercial zirconia powder. Commercial powder has an average particle size of less than 1 micron, while 90 percent of powders have sizes of about 2 microns. Because pre-sintered zirconia powder is ground and recycled by mechanical forces, it has a wider range of particle sizes compared to commercial powder.

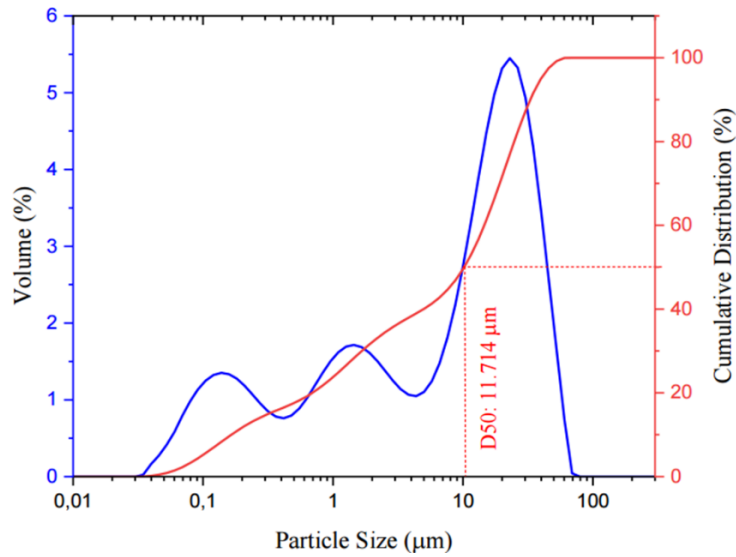


Figure 4.1: Particle size distribution graphs of recycled zirconia powder (R-YSZ)

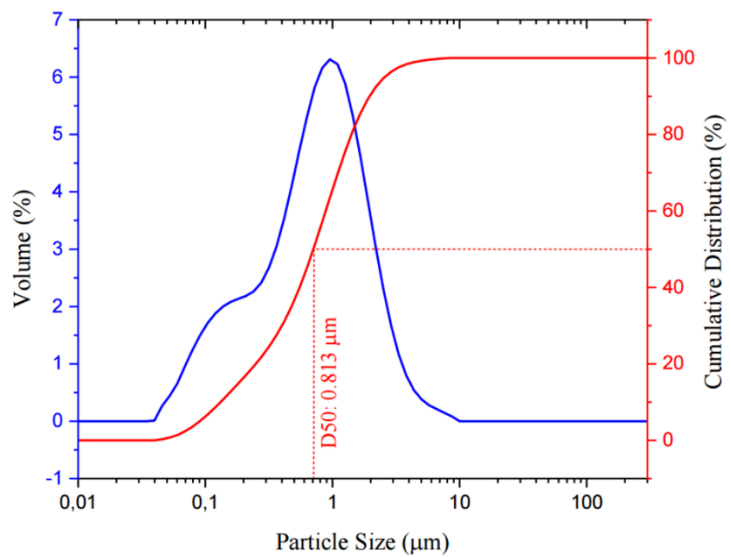


Figure 4.2: Particle size distribution graphs of commercial zirconia powder (COM)

4.1.2 Differential Thermal Analysis Results

Polyvinyl alcohol (PVA) will be used as binder so that the new compositions, which will be formed by doping commercial powder with recycled zirconia in different proportions, will hold together better while being brought into pellet form. When the shaped powders are exposed to high temperature, it is expected that the existing binder will be removed. For this reason, the thermal analysis process was applied to the PVA

to be used as a binder to determine the temperature at which it was completely removed from the body. The TG-DTG curve of PVA is demonstrated in Fig. 4.3.

The initial weight loss for pure PVA occurred between 55-75°C in response to physical water removal. The second weight loss occurs between 219-345°C and this loss corresponds to the thermal degradation of the intermolecular hydrogen bond of PVA. The third degradation between 385-480°C corresponds to the decomposition of the PVA main chain. After a temperature of 506-518°C, the PVA reached a loss of 97% by weight [52,53].

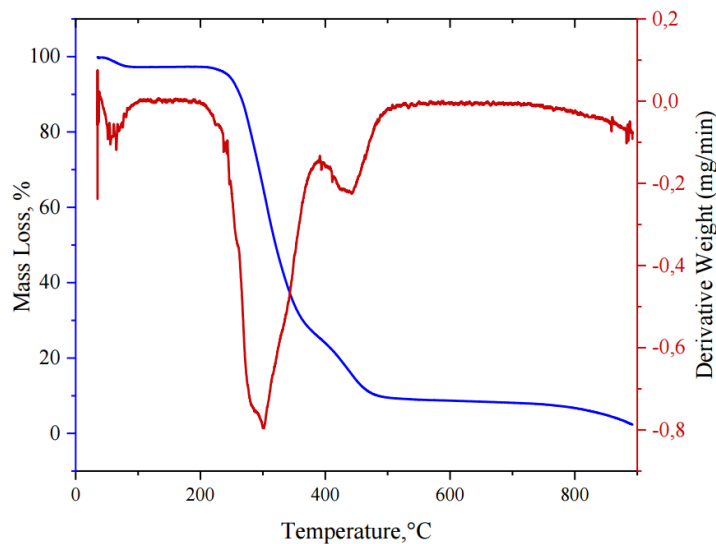


Figure 4.3: TG-DTG curve of polyvinyl alcohol (PVA)

4.1.3 Optical Dilatometer Results

Optical dilatometer analyzes were applied to samples fabricated from commercial powder (COM) and recycled zirconia powder (R-YSZ) to obtain information about the temperature-dependent dimensional changes of the bodies to be produced from raw materials. Before the analysis, the raw material powders were first pressed with the help of a uniaxial press under 55 MPa pressure, then CIPed under 250 MPa pressure. The experiments were carried out by heating the samples from room temperature to 1380°C with a heating rate of 10°C/min and passing them to the cooling stage without waiting at this temperature.

Fig. 4.4 shows the percent expansion of raw materials COM and R-YSZ measured by optical dilatometry. When the graphs were examined, it was observed that the COM sample began to condense at 1197°C. The assay temperature was a maximum of 1380°C and did not show full intensity at this temperature. It has been observed that R-YSZ begins to densify at 1240°C. The fact that R-YSZ starts to dense at a higher temperature rather than COM may be due to the fact that it cannot reach a more bulk form due to reasons such as being obtained from pre-sintered powders, having high particle size, and different powder morphology. These conditions can directly affect to the sintering temperature. At a temperature of 1380°C, which is the maximum capacity of the dilatometer device, a total shrinkage of 16.6% occurred in the COM sample after the experiment, while a shrinkage of 10.6% occurred in the R-YSZ sample. It is understood from the graphs that the temperature of 1380°C for both samples is not sufficient for them to be sintered.

Volpato et al. [21] emphasized the importance of grain size for sintering temperature with dilatometer-measured shrinkage values of nano-sized ZrO₂ and commercial ZrO₂. They stated that the sintering temperature decreased significantly due to the short diffusion distance of nano-structured ZrO₂. In their study, nano-structured ZrO₂ started to condense at 650°C and fully concentrated at 1200°C. Commercial ZrO₂, on the other hand, started to concentrate at 1100°C and began to sinter at 1400°C. Surzhikov et al. [54], in a study on the sintering behavior of ZrO₂, used commercial Tosoh TZ-3Y-E powder, which was also used in this thesis, and applied dilatometric analysis to the sample produced from this powder with a heating rate of 2 C/min. As a result of the analysis, they observed that TZ-3Y-E began to condense at 900-950°C and contracted by about 22% at 1400°C. Considering other similar studies in the literature with 3 mol% yttria doped ZrO₂ [55,56], it was observed that the shrinkage rate of commercial YSZ was 15-20% between 1350-1400°C, and in this thesis study, it was concluded that the shrinkage rates obtained after dilatometric measurements were compatible with the literature. has been reached.

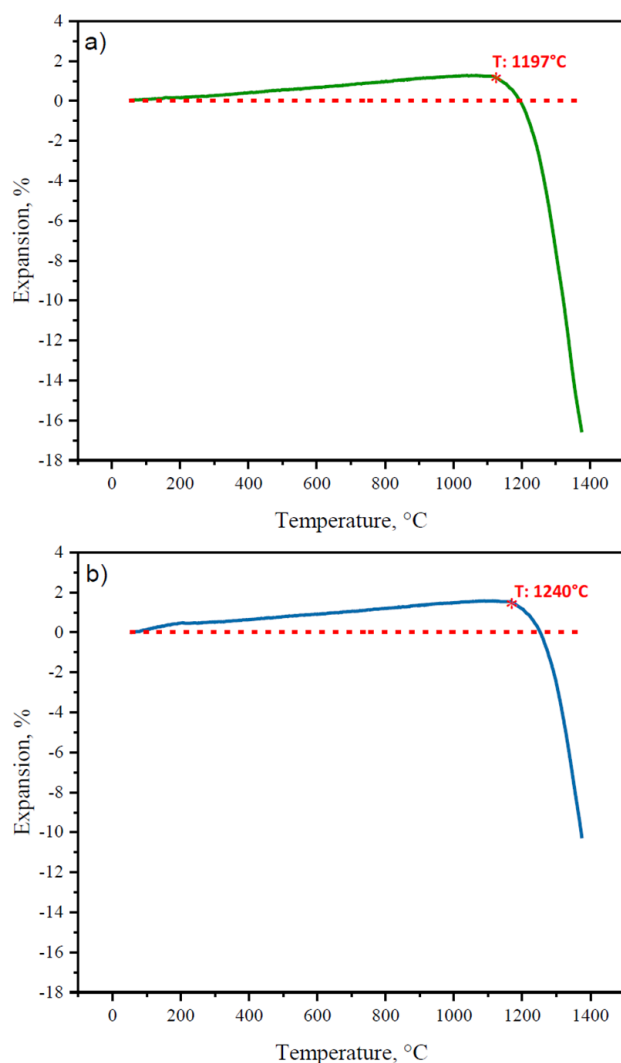


Figure 4.4: Optical dilatometer curves of a) COM, and b) R-YSZ

4.1.4 XRD Analysis Results

The X-ray diffraction patterns of commercial zirconia powder and recycled zirconia powders from pre-sintered waste blocks to be used as raw materials were performed at 2θ intervals of $20\text{--}80^\circ$ and the diffraction pattern obtained are illustrated in Fig. 4.5. Based on these patterns, it was detected that both powders contain tetragonal zirconia as a major phase in agreement with JCPDS card number 01-083-0113. The characteristic peaks of tetragonal ZrO_2 were located at 30.2° , 34.6° , 35.2° , 50.2° , 50.7° , 59.3° , 60.1° and 62.8° corresponding to $t(101)$, $t(34,6)$, $t(35,2)$, $t(112)$, $t(200)$, $t(103)$, $t(211)$, $t(202)$ planes, respectively. Also, it was determined that both powders contain monoclinic zirconia as a minor phase in agreement with JCPDS card number 00-036-

0420, and it was identified that the characteristic peaks of monoclinic ZrO_2 were located at 28.1° and 31.2° corresponding to $m(-111)$ and $m(111)$ planes.

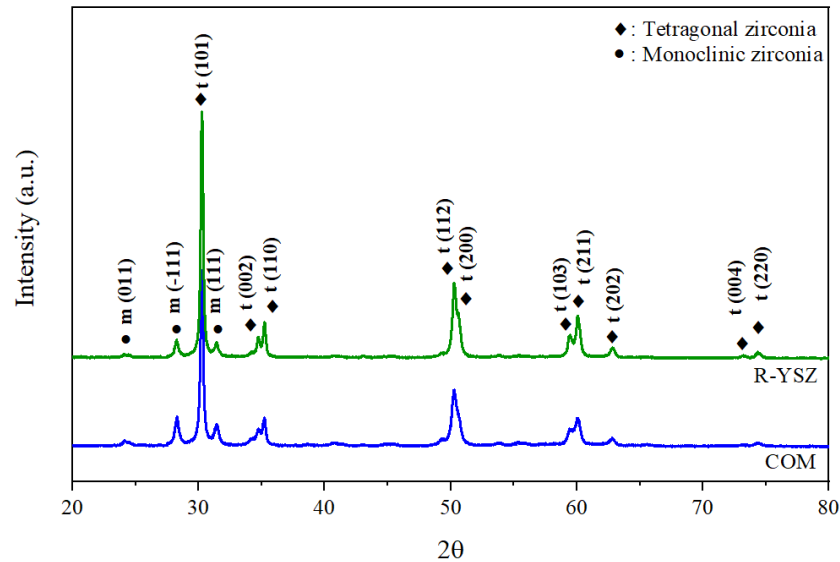


Figure 4.5: XRD patterns of commercial zirconia powder (COM) and recycled zirconia powder (R-YSZ)

4.1.5 SEM Results

Scanning electron microscopy was utilized to observe the morphologies of COM and R-YSZ powders. SEM micrographs of raw materials are given in Fig. 4.6. When the images were examined, it was seen that the commercial powder produced by combining nano-sized zirconia powders with the "spray drying" method had a perfectly spherical form as seen in Fig.4.6(a). The zirconia powder obtained from waste blocks, on the other hand, has the same properties during the production phase, but has gained a different size and morphology due to the mechanical processes it is exposed to during recycling (Fig.4.6(b)). However, the spherical form of the powders has not completely lost its existence.

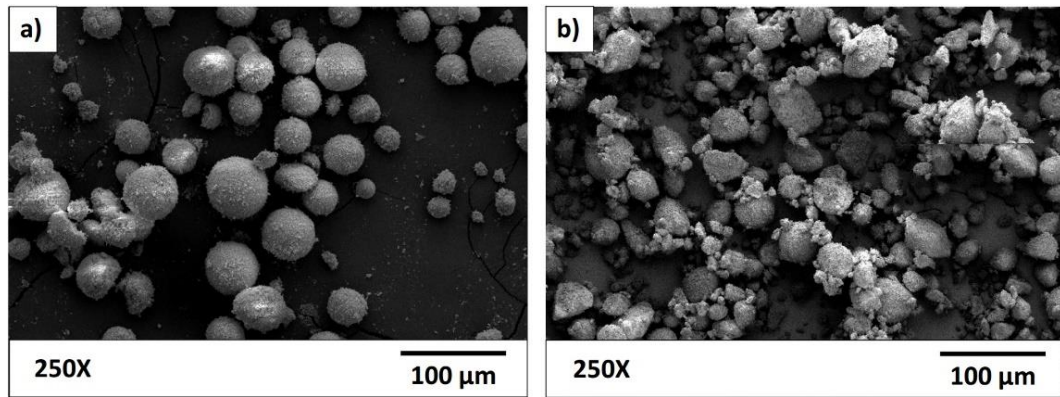


Figure 4.6: SEM micrographs of raw materials, a) COM, b) R-YSZ.

4.2 Characterization Results of Produced Samples

4.2.1 Weight Loss and Dimensional Change Results

The weight and dimensional changes of the samples, which were brought into pellet form after the dry pressing process, were recorded after each applied process. The changes in heights after cold isostatic pressing, pre-sintering and final sintering are listed in Table 4.1. The A-CIP specified in the table represents the percentage of change in height after cold isostatic pressing. During the CIP process, since a load of 250 MPa was applied to the samples shaped under 55 MPa load, a change of approximately 1.5% occurred in the dimensions of the samples due to high loading, even without heat treatment. After the pre-sintering process applied to all samples at the same temperature and dwelling time, a change of approximately 2% occurred. Considering the results after the final sintering, a change of approximately 20% occurs for all temperatures, while these changes show slight differences for different compositions and temperatures. Increasing the sintering temperature contributed to the relative increase in dimensional change in some compositions.

Table 4.1: The linear shrinkage of samples

Sample Code	A-CIP	Pre-Sintering		Full Sintering	
	Room Temp.	1000°C	1450°C	1500°C	1550°C
COM	1.94 ± 0.02	1.77 ± 0.32	20.56 ± 0.61	19.71 ± 0.36	20.11 ± 0.18
3R-YSZ	2.12 ± 0.08	2.20 ± 0.38	19.08 ± 0.43	18.95 ± 0.22	19.66 ± 0.34
5R-YSZ	1.18 ± 0.57	1.73 ± 0.76	19.01 ± 0.32	19.45 ± 0.32	19.38 ± 0.09
10R-YSZ	1.20 ± 0.78	1.98 ± 0.99	19.41 ± 0.36	19.85 ± 0.32	19.82 ± 0.72
15R-YSZ	1.11 ± 0.65	2.04 ± 0.77	19.94 ± 0.17	19.51 ± 0.33	19.55 ± 0.21
30R-YSZ	1.48 ± 0.87	2.01 ± 0.82	18.61 ± 0.23	18.78 ± 0.42	19.32 ± 0.48
50R-YSZ	1.29 ± 0.48	1.79 ± 0.82	19.74 ± 0.11	19.29 ± 0.31	19.47 ± 0.21
100R-YSZ	1.31 ± 0.60	2.32 ± 1.03	19.50 ± 0.33	19.62 ± 0.43	20.05 ± 0.77

* Linear shrinkage: %

Table 4.2 shows the amount of reduction in the diameters of the samples in percent at each production step. After cold isostatic pressing, there is a decrease of approximately 2.5% in the diameters of the samples, while after the pre-sintering process, there is a total decrease of approximately 3% in the diameters of the samples compared to their initial state. Although the decrease in diameter of the samples, which became denser with high temperature, was 22.5%, it was observed that this value decreased to 21.5% with the increase in the amount of waste zirconia additive.

The percent values of weight reduction are listed in Table 4.3. The weight loss after CIP is due to the adhesion of the powders to the vacuum environment under the influence of high pressure and deformation under the influence of high pressure. In addition, the removal of moisture from the body over time in the environment where it waits until the pre-sintering process also causes weight loss. After the pre-sintering process, it was calculated that an average of 1.35% weight loss occurred in all samples. This is due to the removal of the binder from the body during pre-sintering. In the final sintering processes, the weight loss is significantly less. A relative increase in weight loss was observed with increasing additive amount. Contaminations thought to be present in recycled zirconia powder may be the reason for this increase.

Table 4.2: The percent diameters change of samples

Sample Code	A-CIP	Pre-Sintering		Full Sintering	
	Room Temp.	1000°C	1450°C	1500°C	1550°C
COM	2.60 ± 0.24	2.97 ± 0.25	22.60 ± 0.05	22.63 ± 0.48	22.87 ± 0.13
3R-YSZ	2.95 ± 0.37	3.06 ± 0.27	22.56 ± 0.19	22.81 ± 0.30	23.07 ± 0.22
5R-YSZ	2.88 ± 0.36	3.02 ± 0.33	22.58 ± 0.08	22.91 ± 0.33	23.18 ± 0.18
10R-YSZ	2.95 ± 0.34	3.17 ± 0.31	22.52 ± 0.24	22.89 ± 0.21	22.92 ± 0.06
15R-YSZ	2.99 ± 0.84	2.74 ± 0.17	22.24 ± 0.16	22.44 ± 0.39	22.72 ± 0.55
30R-YSZ	2.70 ± 0.59	2.93 ± 0.46	22.21 ± 0.80	22.14 ± 0.18	22.67 ± 0.54
50R-YSZ	2.38 ± 0.28	2.96 ± 0.24	22.09 ± 0.11	22.45 ± 0.25	22.70 ± 1.57
100R-YSZ	1.79 ± 0.29	2.38 ± 0.53	21.57 ± 0.30	22.08 ± 0.15	21.57 ± 0.24

Table 4.3: The percent weight loss of samples.

Sample Code	A-CIP	Pre-Sintering		Full Sintering	
	Room Temp.	1000°C	1450°C	1500°C	1550°C
COM	0.10 ± 0.06	0.42 ± 0.03	0.27 ± 0.00	0.27 ± 0.01	0.28 ± 0.01
3R-YSZ	1.14 ± 1.09	0.56 ± 0.22	0.28 ± 0.01	0.27± 0.01	0.27± 0.01
5R-YSZ	1.23 ± 0.80	1.64 ± 1.48	0.28 ± 0.59	0.27± 0.01	0.26± 0.01
10R-YSZ	1.93 ± 1.21	1.37 ± 1.13	0.26 ± 0.01	0.27± 0.01	0.27± 0.01
15R-YSZ	1.33 ± 1.01	2.13 ± 1.54	0.28 ± 0.02	0.29 ± 0.01	0.27± 0.01
30R-YSZ	2.01 ± 1.58	1.54 ± 1.23	0.32 ± 0.01	0.33 ± 0.01	0.33 ± 0.01
50R-YSZ	1.77 ± 1.50	0.96 ± 0.32	0.37 ± 0.03	0.37 ± 0.02	0.35 ± 0.01
100R-YSZ	2.96 ± 0.76	2.03 ± 1.84	0.41 ± 0.01	0.40 ± 0.01	0.40 ± 0.04

Table 4.4 lists the dimensional density values of the samples. Dimensional density results give average values and open porosities that exist in the body are also included. When these density values measured using the diameter, height and weights of the samples were examined, it was observed that the density values obtained after cold isostatic pressing and after pre-sintering gave very close results. After pre-sintering,

the dimensional densities of the samples are $\sim 3 \text{ gr/cm}^3$ and the standard deviation values are quite low. With the effect of high temperature in the full sintering steps, the samples gained a denser state, and the COM sample reached a density of 6 g/cm^3 at all sintering temperatures. In the samples affected by the losses in weight, diameter and height, the dimensional density values tended to decrease as the waste zirconia additive ratio increased within the body. While there is no significant loss in density up to the 30R-YSZ sample, a decrease in dimensional density values is noticeable after this waste additive ratio. Such that, a density difference of 2.5% was detected between the 100R-YSZ sample and the COM sample.

Table 4.4: The average dimensional volumes of samples

Sample Code	A-CIP	Pre-Sintering			Full Sintering	
	Room Temp.	1000°C	1450°C	1500°C	1550°C	
COM	2.92 ± 0.05	3.08 ± 0.01	6.02 ± 0.02	6.03 ± 0.07	6.06 ± 0.01	
3R-YSZ	2.92 ± 0.07	3.07 ± 0.01	5.99 ± 0.04	5.98 ± 0.02	6.05 ± 0.03	
5R-YSZ	2.97 ± 0.10	3.06 ± 0.02	5.97 ± 0.04	6.06 ± 2.42	6.05 ± 0.02	
10R-YSZ	2.96 ± 0.09	3.06 ± 0.01	5.99 ± 0.03	6.02 ± 2.41	6.03 ± 0.01	
15R-YSZ	2.98 ± 0.13	3.07 ± 0.01	5.99 ± 0.04	5.98 ± 2.39	6.04 ± 0.02	
30R-YSZ	2.99 ± 0.12	3.09 ± 0.01	5.95 ± 0.02	5.97 ± 0.02	6.01 ± 0.06	
50R-YSZ	2.95 ± 0.06	3.04 ± 0.01	5.91 ± 0.01	5.93 ± 0.01	6.02 ± 0.10	
100R-YSZ	3.01 ± 0.10	3.00 ± 0.01	5.87 ± 0.05	5.87 ± 0.03	5.89 ± 0.03	

* Average dimensional volumes: gr/cm^3

4.2.2 Density Measurements Results

Archimedes test was applied to calculate the bulk densities, apparent specific gravity and percent apparent porosity values of the pre-sintered original block and the produced samples, after pre-sintering and full sintering processes. The reason for including the original block in this experiment is to compare how close we can get to

the density results of this pre-sintered block, which is sold commercially to dental laboratories, in the samples we produce. Bulk density results with standard deviation values for all samples are listed in Table 4.5. The bulk density values of OB, COM and 100R-YSZ samples after pre-sintering are relatively close to each other and are approximately 3 gr/cm³. Similar results were observed in other samples added with recycled zirconia. At the sintering temperature of 1450°C, the bulk density value is the lowest in the 100R-YSZ sample with 5.5 gr/cm³. This value is 5.98 gr/cm³ for OB sample.

As the amount of recycled zirconia additive increased, the bulk density values decreased significantly. This situation also occurred at increasing sintering temperatures, but since the body becomes denser with the effect of temperature, there was an increase in bulk density. The density value required for surgical implant applications is defined as a density equal to or greater than 6.00 g/cm³ in the ASTM F1873-98 Standard [57]. High bulk density values in accordance with the standard have been achieved, up to 30% recycled zirconia additive ratio at 1550°C, considering the standard deviation values. Likewise, in samples sintered at 1500°C, results close to this value could be obtained with an additive ratio of up to 15%.

Table 4.5: Bulk density of pre-sintered and sintered samples.

Sample Code	Pre-Sintering		Full Sintering	
	1000°C	1450°C	1500°C	1550°C
OB	3.014	5.984	5.985	6.015
COM	3.13 ± 0.03	5.66 ± 0.07	5.98 ± 0.02	6.02 ± 0.02
3R-YSZ	3.10 ± 0.02	5.68 ± 0.04	5.97 ± 0.04	5.99 ± 0.03
5R-YSZ	3.10 ± 0.00	5.65 ± 0.01	5.95 ± 0.04	6.02 ± 0.02
10R-YSZ	3.07 ± 0.10	5.71 ± 0.03	5.94 ± 0.06	6.01 ± 0.01
15R-YSZ	3.09 ± 0.06	5.77 ± 0.02	5.95 ± 0.01	5.99 ± 0.01
30R-YSZ	3.09 ± 0.01	5.68 ± 0.02	5.88 ± 0.05	5.96 ± 0.04
50R-YSZ	3.06 ± 0.02	5.70 ± 0.06	5.88 ± 0.02	5.95 ± 0.02
100R-YSZ	2.99 ± 0.01	5.51 ± 0.07	5.73 ± 0.09	5.77 ± 0.04

*Bulk density: gr/cm³

Akimov [58] reported that the increase in CIP compression pressure in the correct sintering regime is an important factor in increasing the density and strength of ceramics. According to this literature data, 250 MPa CIP pressure was sufficient to obtain density results in accordance with the standard at 1550°C sintering temperature, but it is necessary to increase the CIP compression pressure to reach sufficient density values at other sintering temperatures.

Apparent specific gravity is the ratio of the weight of a volume of the substance to the weight of an equal volume of the reference substance. This ratio is known also as the volume weight. According to the formula in Equation (3.3), since the units of weights cancel each other, the term specific gravity becomes a dimensionless quantity. The apparent specific gravity of the samples is listed in Table 4.6. When the table is examined, it is seen that the apparent specific gravity results at the full sintering temperatures are quite close to each other. This is because the apparent specific gravity does not contain permeable, that is, open pores. The results are close to each other, as the situation is almost equal when the weight of the open pores in the body is eliminated.

Table 4.6: Apparent specific gravity of pre-sintered and sintered samples

Sample Code	Pre-Sintering		Full Sintering	
	1000°C	1450°C	1500°C	1550°C
OB	5.83	6.04	6.04	6.06
COM	6.06 ± 0.09	6.06 ± 0.02	6.03 ± 0.01	6.06 ± 0.01
3R-YSZ	6.02 ± 0.02	6.11 ± 0.03	6.05 ± 0.01	6.07 ± 0.01
5R-YSZ	5.99 ± 0.01	6.06 ± 0.01	6.03 ± 0.01	6.07 ± 0.01
10R-YSZ	5.80 ± 0.23	6.07 ± 0.02	6.03 ± 0.01	6.07 ± 0.01
15R-YSZ	6.31 ± 0.60	6.06 ± 0.02	6.04 ± 0.02	6.07 ± 0.01
30R-YSZ	5.97 ± 0.03	6.05 ± 0.02	6.05 ± 0.02	6.05 ± 0.01
50R-YSZ	5.97 ± 0.03	6.03 ± 0.01	6.02 ± 0.01	6.04 ± 0.01
100R-YSZ	5.97 ± 0.01	5.99 ± 0.01	6.01 ± 0.01	6.01 ± 0.01

The apparent porosities of the samples after pre-sintering and full sintering are given in Table 4.7. Apparent porosity expresses the volume of open pores in the sample as a percentage relative to its external volume [59]. Considering the results, it was determined that the samples contained 48-50% pores after pre-sintering. Compared to other sintering temperatures, it was observed that the OB sample sintered at 1450°C and the samples added with recycled zirconia had higher porosity. While the pore percentages of the samples, which gained a denser structure with the increase in temperature, tended to decrease, the increasing amount of recycled zirconia additive caused the porosity percentage to increase at all sintering temperatures. At 1500°C and 1550°C sintering temperatures, results compatible with OB were obtained up to 10% additive ratio.

Table 4.7: Apparent porosity of pre-sintered and sintered samples

Sample Code	Pre-Sintering		Full Sintering	
	1000°C	1450°C	1500°C	1550°C
OB	48.33	4.49	0.84	0.80
COM	48.37 ± 0.31	6.69 ± 1.49	0.82 ± 0.17	0.60 ± 0.25
3R-YSZ	48.50 ± 0.21	7.02 ± 0.70	1.42 ± 0.53	0.76 ± 0.39
5R-YSZ	48.31 ± 0.08	6.78 ± 0.23	1.51 ± 0.63	0.80 ± 0.23
10R-YSZ	46.95 ± 3.44	5.93 ± 0.24	2.02 ± 1.15	1.00 ± 0.10
15R-YSZ	50.54 ± 5.29	4.82 ± 0.29	1.40 ± 0.36	1.25 ± 0.13
30R-YSZ	48.28 ± 0.28	6.04 ± 0.63	2.75 ± 1.09	1.59 ± 0.58
50R-YSZ	48.71 ± 0.11	5.47 ± 1.21	2.42 ± 0.14	1.55 ± 0.11
100R-YSZ	49.98 ± 0.22	8.06 ± 1.08	4.41 ± 1.45	3.76 ± 0.63

*Apparent porosity: %

4.2.3 XRD Results

X-ray phase analyzes of ceramic samples sintered at 1450°C, 1500°C and 1550°C temperatures were performed at 2θ intervals of 20–80° and the obtained diffraction

patterns are shown in Fig. 4.7, Fig. 4.8, and Fig. 4.9, respectively. All samples sintered at different temperatures exhibited almost identical diffraction patterns. It was detected that all samples contain tetragonal zirconia in agreement with JCPDS card number 01-083-0113. The characteristic peaks of tetragonal ZrO_2 were located at 30.2° , 34.6° , 35.2° , 50.2° , 50.7° , 59.3° , 60.1° , and 62.8° corresponding to $t(101)$, $t(002)$, $t(110)$, $t(112)$, $t(200)$, $t(103)$, $t(211)$, $t(202)$ planes, respectively.

None of the samples sintered at 1450°C and 1500°C demonstrated peaks of the monoclinic (m) ZrO_2 phase that existed before sintering. However, in all of the samples sintered at 1550°C , it was observed that a peak occurred at 28.19° , consistent with the characteristic peak of the (m) ZrO_2 phase with JCPDS card number 00-036-0420. The (m) ZrO_2 phase is represented by an “•” on the figure. Chen et al. [60] also encountered the formation of monoclinic phase at these temperatures and reported that this situation may cause loss of transformation-hardening mechanism and severe deterioration of mechanical properties.

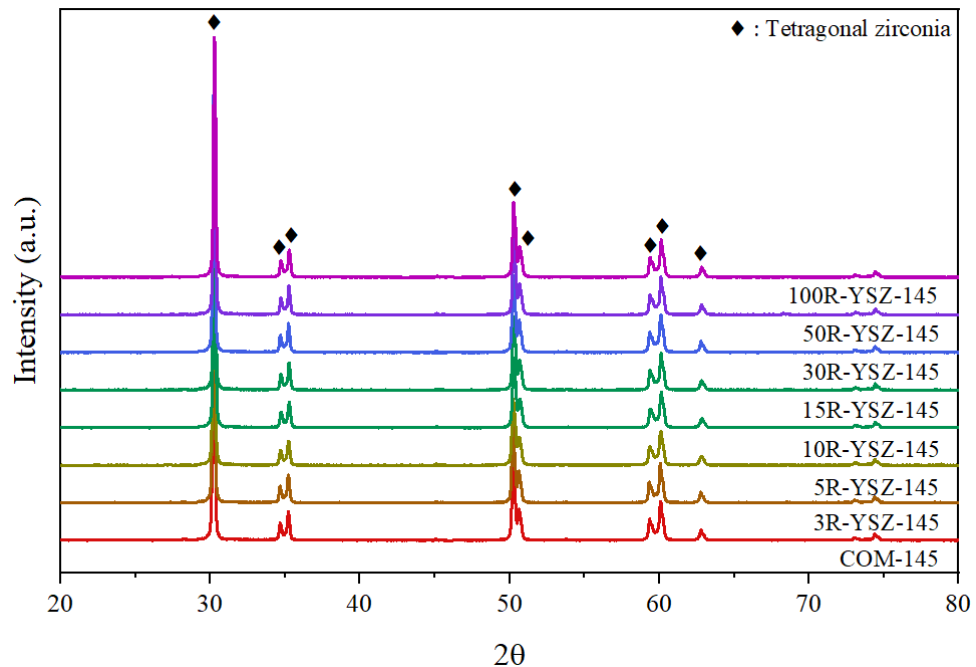


Figure 4.7: XRD patterns of samples sintered at 1450°C

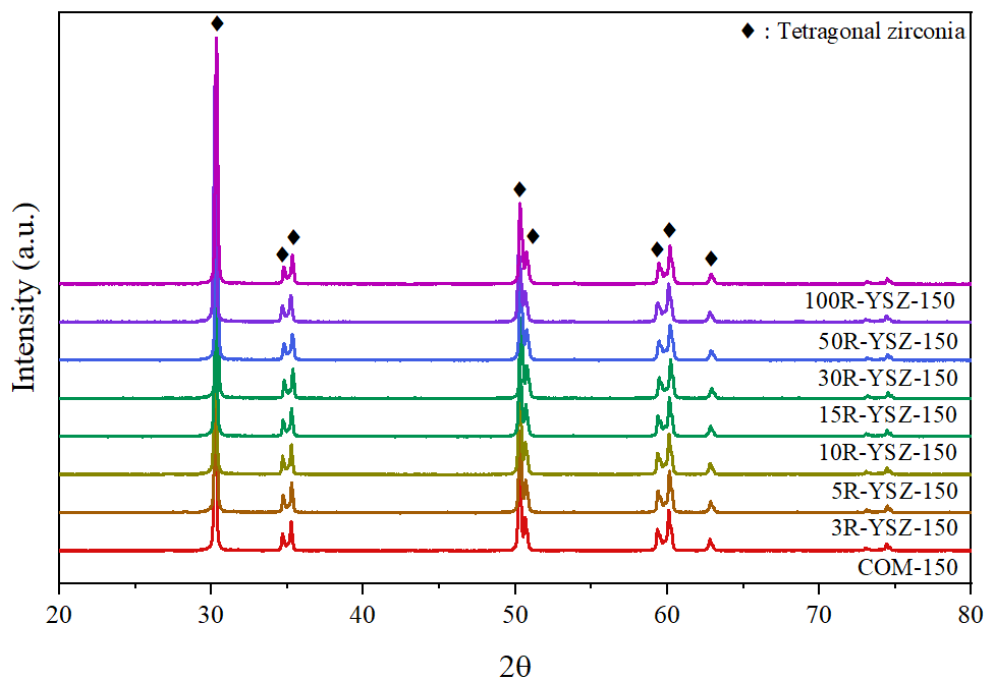


Figure 4.8: XRD patterns of samples sintered at 1500°C

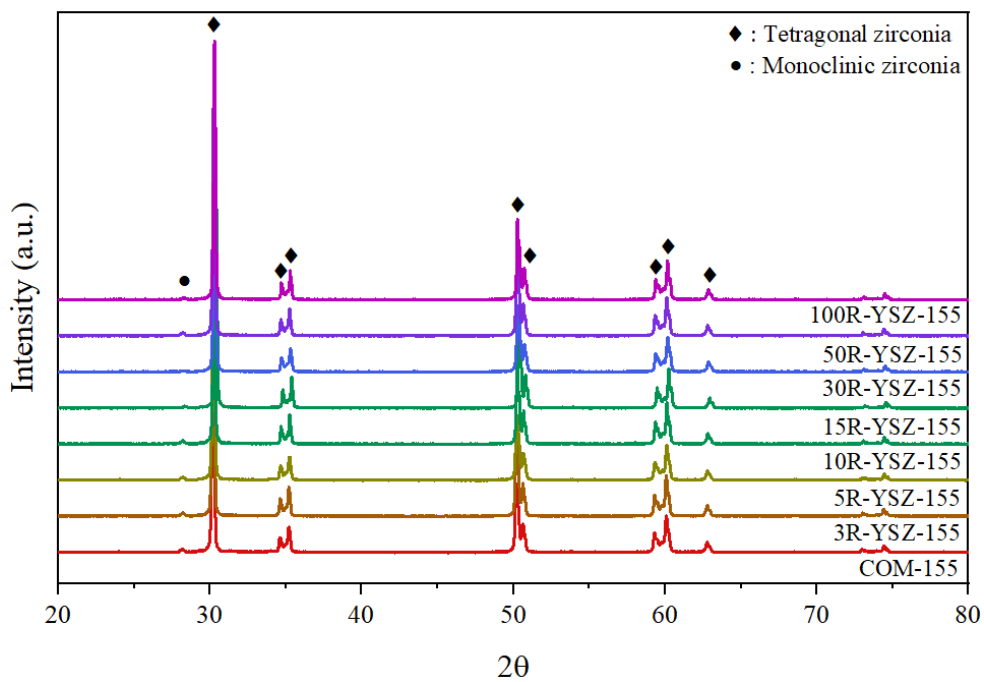


Figure 4.9: XRD patterns of samples sintered at 1550°C

4.2.4 Low Temperature Degradation Test Results

All samples sintered at 1450°C, 1500°C and 1550°C were hydrothermally aged for 5 hours, 10 hours and 15 hours. After the aging process, X-ray analysis was applied to the metallographically prepared surfaces before the experiment. The graphs given in the results of XRD analysis, where we can observe the interaction of sintering temperature and waste additive ratio with aging time on 5R-YSZ with low waste additive ratio, and fully recycled 100R-YSZ (or R-YSZ) samples. The XRD patterns of the 5R-YSZ and 100R-YSZ samples were shared at intervals of 27-37° in order to clearly see the changes in the peak intensities. When the images in Fig. 4.10 and Fig. 4.11 are examined, as a result of aging processes, it is observed that monoclinic $m(-111)$, $m(111)$ and $m(002)$ peaks are located at 2θ of 28.19°, 31.48° and 34.19°, respectively. While a significant increase was observed in monoclinic phase percentages with increasing aging time, it was observed that the intensities of tetragonal $t(101)$, $t(002)$, and $t(110)$ peaks tended to decrease. This phenomenon demonstrated its effect more with increasing sintering temperature. As sintering temperature and aging time increased, monoclinic phase peak intensities increased and tetragonal phase peak intensities decreased. Amat et al. [61] stated that this is due to grain growth occurring at high sintering temperature. When the grain size increases, an initial tetragonal-monoclinic transformation might be initiated due to the thermal stress of sintering. They also stated that in addition to grain growth, intergranular porosity can increase this transformation. Kosmac et al. [62] stated that after in vitro aging, zirconium phase densities were related to starting powder, sintering temperature and aging time. Inokoshi et al. [63], on the other hand, concluded in their study that sintering at high temperatures and long dwelling times significantly affect grain growth, which in turn causes an increase in the amount of phase percentage of monoclinic ZrO_2 .

Graphs illustrating percent monoclinic phase fractions according to the sintering temperature of all hydrothermally aged samples are given in Fig. 4.12, Fig. 4.13 and Fig. 4.14. The 25% monoclinic ZrO_2 content, which is determined by the ISO 13356:2008 standard [25] as the limit for the use as dental materials, is indicated as a border line in all graphics and the area above this limit is indicated as shaded.

According to Fig. 4.12, after 5 hours of aging, it was observed that 100R-YSZ-145 sample contained 8.2% monoclinic phase, and this value was between 3.5% and 5.5% for all remaining samples. In the samples aged at different times, as the aging time increased, there was a noticeable increase in the m-ZrO₂ phase contents, as can be seen in the peak intensities in the XRD graphs.

Except for 100R-YSZ-150, all samples sintered at 1500°C were observed to have less than 25% monoclinic phase content at all aging times (as seen in Fig. 4.13). Although all other samples were still below the limit at 5 hours and 10 hours, only the 5R-YSZ and 10R-YSZ samples slightly exceeded the limit with 26.5% monoclinic phase content at the end of 15 aging periods.

All samples except 100R-YSZ, which were sintered at 1550°C, had a monoclinic phase content of 7% to 13% after 5 hours of aging. This range meets the requirements of the ISO 13356:2008 standard. However, it is seen that the percentage of monoclinic phase increases significantly at the end of the aging process of 10 hours and 15 hours (Fig. 4.14).

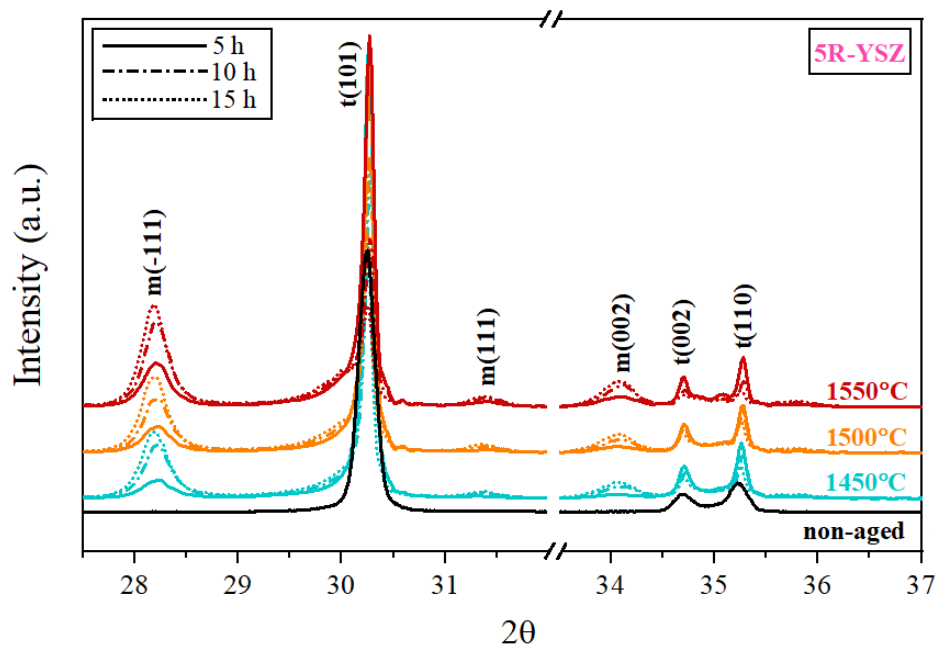


Figure 4.10: XRD patterns of samples sintered at 1450°C, 1500°C, and 1550°C, after aging process for 5h, 10h and 15h

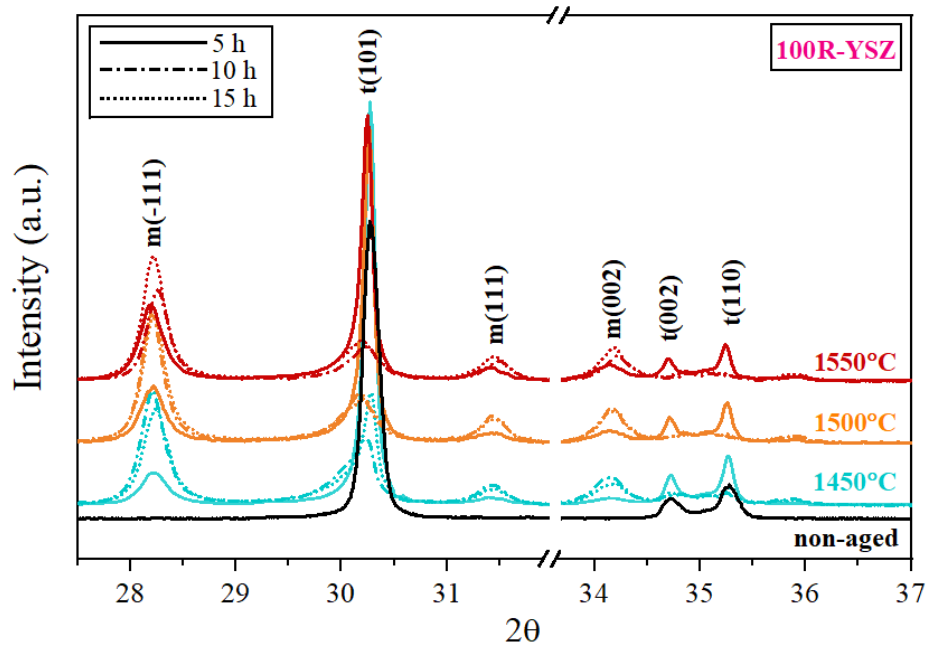


Figure 4.11: XRD patterns of samples sintered at 1450°C, 1500°C, and 1550°C, after aging process for 5h, 10h and 15h

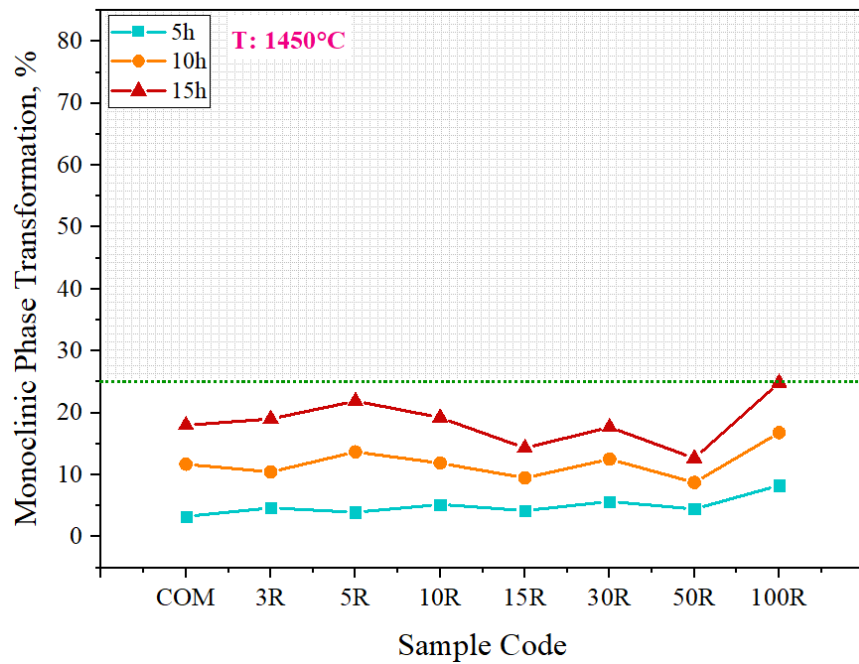


Figure 4.12: Percent monoclinic phase transformation of samples sintered at 1450°C, after aging process for 5h, 10h and 15h

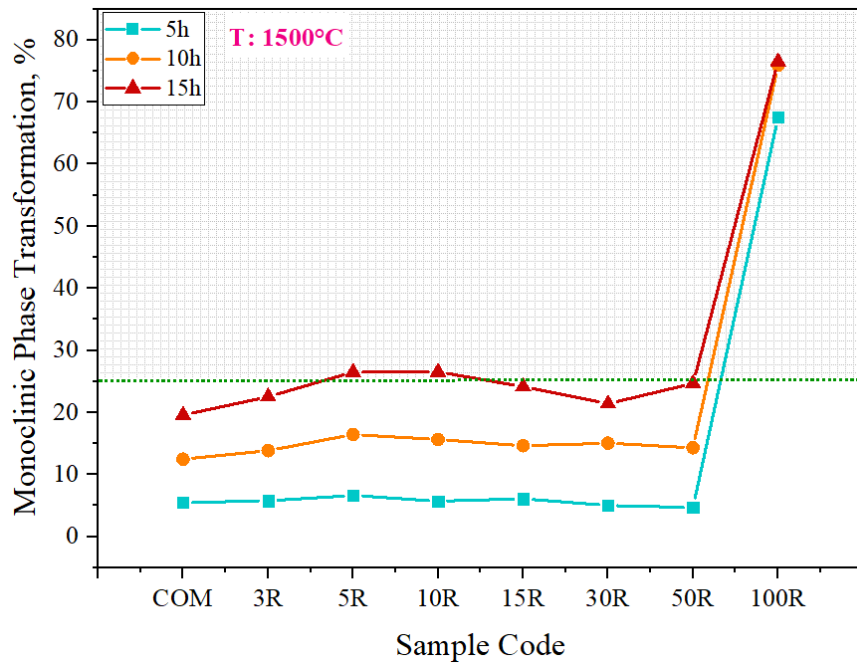


Figure 4.13: Percent monoclinic phase transformation of samples sintered at 1500°C, after aging process for 5h, 10h and 15h

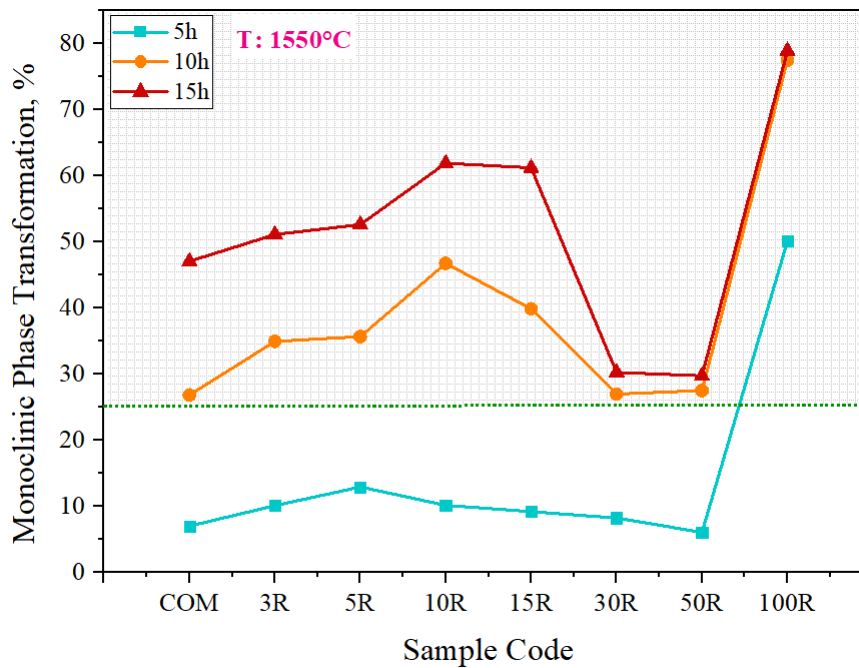


Figure 4.14: Percent monoclinic phase transformation of samples sintered at 1550°C, after aging process for 5h, 10h and 15h

4.2.5 SEM Results

In order to examine the effect of sintering temperature on microstructure, all samples sintered for 2 hours at 1450°C, 1500°C and 1550°C were analyzed by SEM. Images taken at 20000 magnifications are shown in Fig. 4.15, Fig. 4.16 and Fig. 4.17. It was observed that the grain sizes of all samples exhibit similar properties with each other when compared considering their sintering temperatures. It can be seen that the grains of the samples for all sintering temperatures are below 1 μm and have a homogeneous distribution. The increasing the sintering temperature led to a noticeable grain growth in all compositions.

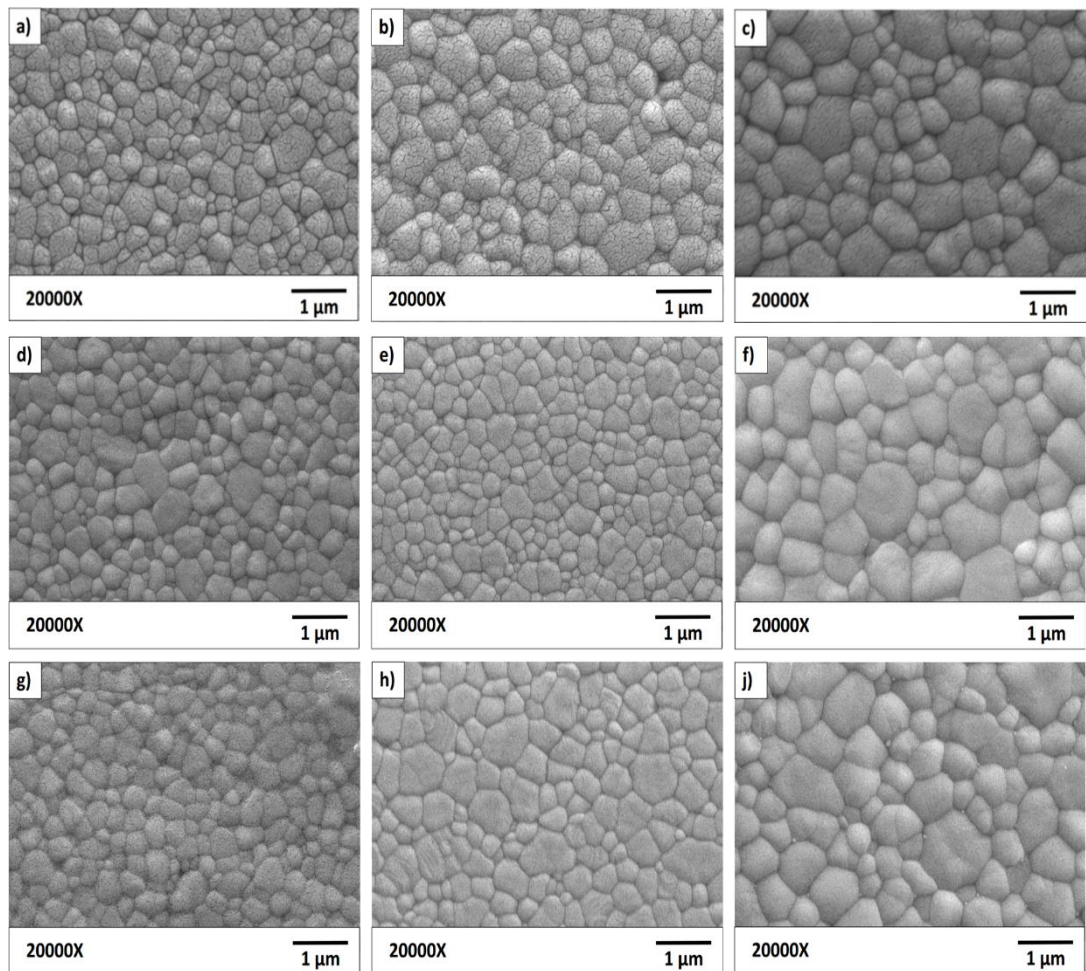


Figure 4.15: SEM images of OB, COM, and 3R-YSZ samples, a) OB-145, b) OB-150 c) OB-155, d) COM-145, e) COM-150, f) COM-155, g) 3R-YSZ-145, h) 3R-YSZ-150, j) 3R-YSZ-155

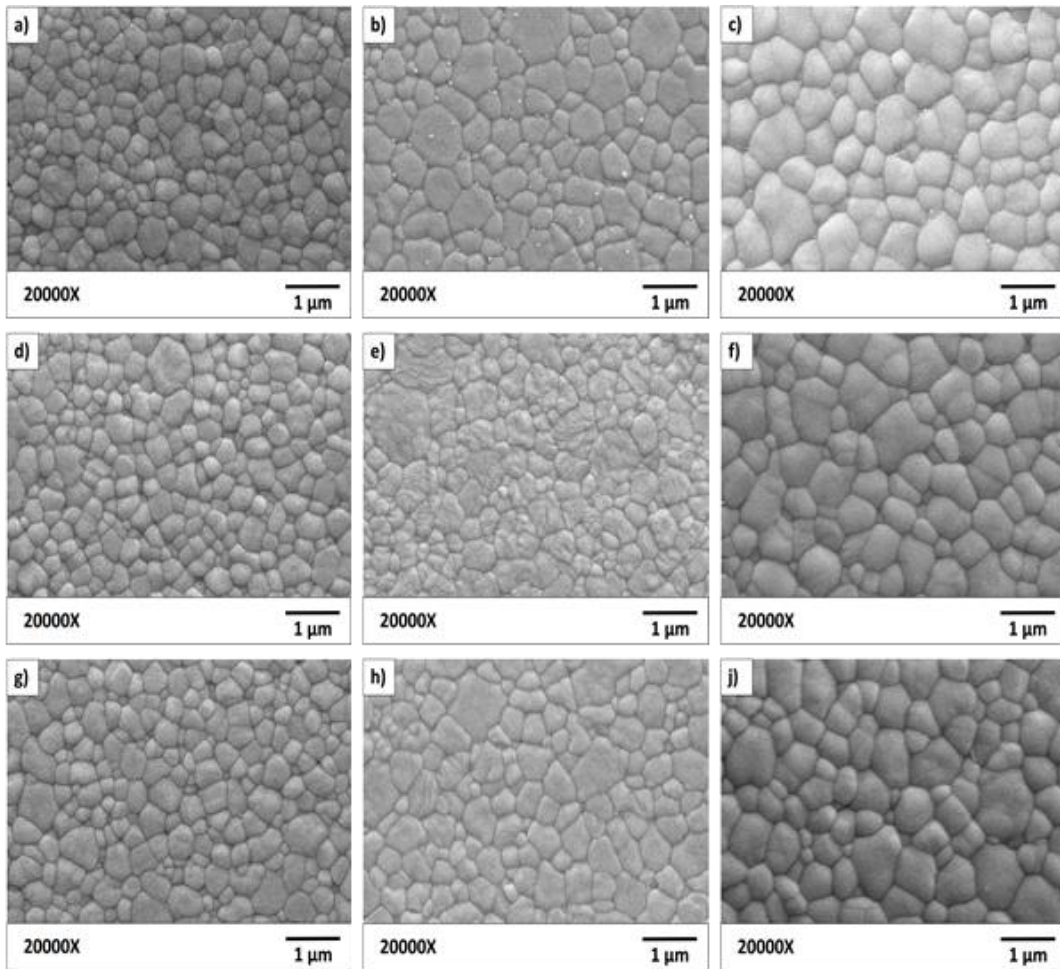


Figure 4.16: SEM images of 5R-YSZ, 10R-YSZ and 15R-YSZ samples, a) 5R-YSZ-145, b) 5R-YSZ-150 c) 5R-YSZ-155, d) 10R-YSZ-145, e) 10R-YSZ-150, f) 10R-YSZ-155, g) 15R-YSZ-145, h) 15R-YSZ-150, j) 15R-YSZ-155

Nilüfer [4] reported that abnormal grain growth was observed at different sintering temperatures in his own study and in some studies with Y-TZP in the literature. However, excessive grain growth did not occur in any sample produced in present study. The linear intersection method was used to determine the average grain size and to calculate the amount of growth in grain size with the effect of sintering temperature. For this method, the rules set by the EN-623-3 standard for advanced technical ceramics were applied. The standard recommends drawing at least five straight lines with random position and orientation along each micrograph intersecting at least 100 grains and averaging the number of points of intersection of grain and lines after multiplying by various coefficients. In order to reach the determined grain number, the

method was applied on micrographs with 5000 magnifications. The mean grain sizes of all samples calculated using the linear intercept method are listed in Table 4.8 with their standard deviation values.

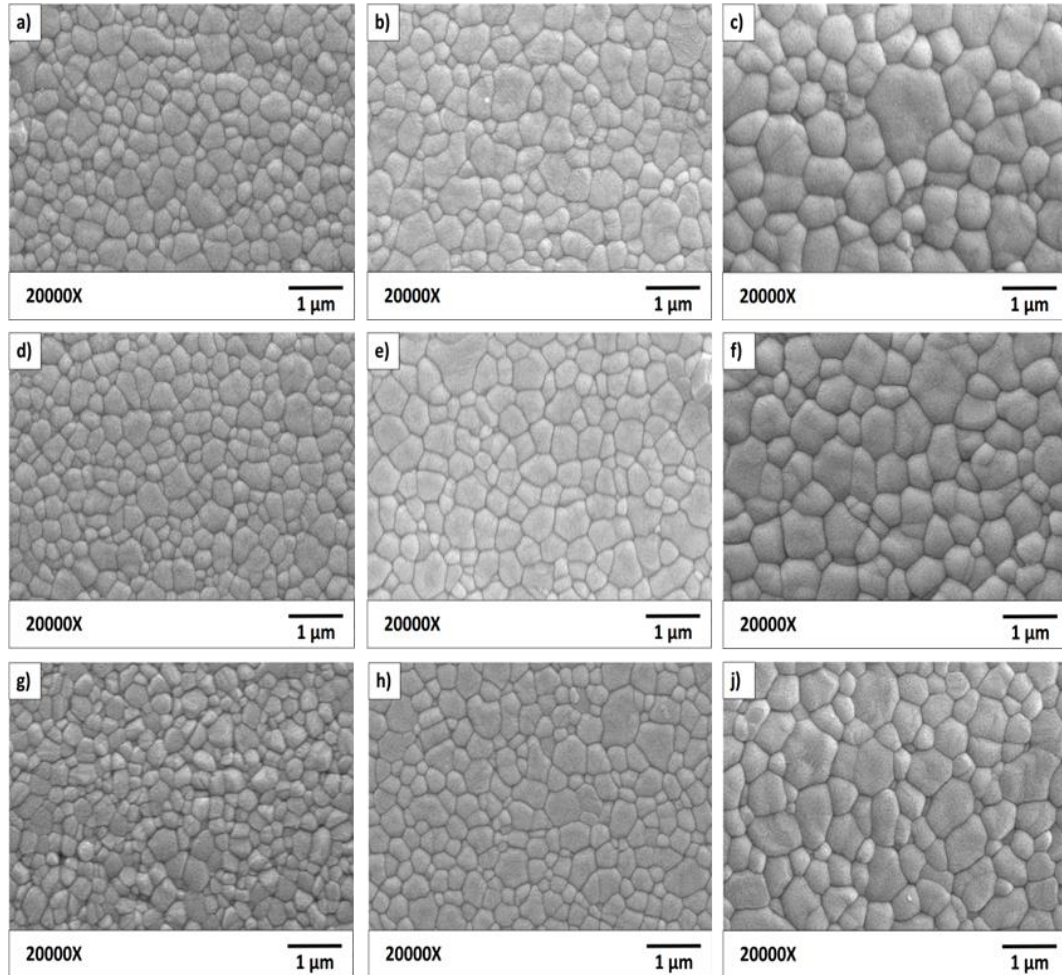


Figure 4.17: SEM images of 30R-YSZ, 50R-YSZ and 100R-YSZ samples, a) 30R-YSZ-145, b) 30R-YSZ-150 c) 30R-YSZ-155, d) 50R-YSZ-145, e) 50R-YSZ-150, f) 50R-YSZ-155, g) 100R-YSZ-145, h) 100R-YSZ-150, j) 100R-YSZ-155

It was calculated that the average grain size of the samples sintered at 1450°C was approximately 0.32 μm , the average grain size of the samples sintered at 1500°C was $\sim 0.41 \mu\text{m}$, and the average grain size of the samples sintered at 1550°C finally was $\sim 0.56 \mu\text{m}$. Consistent with the SEM micrographs, the grains of the samples grew as the sintering temperature increased. Gouveia et al. [37] used Tosoh commercial powder in a similar study and declared that the average grain size range reported by

the manufacturer for the 1500°C sintering condition was approximately 0.4 μm . In this case, it can be said that the average grain size values obtained at the sintering temperatures of 1450°C and 1500°C in this study are suitable for the usage range determined by the manufacturer.

Table 4.8: Average grain sizes of sintered samples

Sample Code	Full Sintering		
	1450°C	1500°C	1550°C
OB	0,36 \pm 0,04	0,40 \pm 0,03	0,65 \pm 0,03
COM	0,34 \pm 0,04	0,40 \pm 0,03	0,64 \pm 0,05
3R-YSZ	0,32 \pm 0,03	0,44 \pm 0,07	0,54 \pm 0,09
5R-YSZ	0,33 \pm 0,03	0,44 \pm 0,06	0,56 \pm 0,08
10R-YSZ	0,31 \pm 0,04	0,44 \pm 0,23	0,50 \pm 0,07
15R-YSZ	0,34 \pm 0,04	0,45 \pm 0,06	0,50 \pm 0,06
30R-YSZ	0,31 \pm 0,03	0,41 \pm 0,04	0,59 \pm 0,11
50R-YSZ	0,32 \pm 0,04	0,40 \pm 0,04	0,54 \pm 0,09
100R-YSZ	0,27 \pm 0,02	0,32 \pm 0,10	0,51 \pm 0,04

* Average grain size: μm (micrometer).

Samples produced with the original block (OB) and commercial powder (COM) exhibited so close average grain size values at all sintering temperatures. In addition, samples containing up to 50% recycled zirconia (50R-YSZ) sintered at 1450°C and 1500°C similarly showed results close to the average grain sizes of the OB and COM samples. However, at these temperatures, the 100R-YSZ (100% recycled zirconia) sample had a smaller grain size than the OB and COM samples. In the samples sintered at 1550°C, approximately 42% grain growth occurred compared to 1450°C. OB-155 and COM-155 samples have the highest grain size values at this temperature. The grain size of the 100R-YSZ-155 sample is approximately 20% lower than the OB-155 and COM-155 samples.

Masahiro Kamiya et al. [36] concluded in their study that the post-sinter grain size of yttria-doped zirconia powders recovered by hydrothermal method is larger than commercial powders. They reported that the reason for this was that the recycled powders could not be ground finer than the primary particles. However, in another study, it was found that zirconia powder recycled by being exposed to mechanical forces for a long time has a smaller grain size than commercial powder. It has been confirmed by the results obtained that the samples (100R-YSZ) produced from recycled zirconia powder produced within the scope of this thesis and sintered at 1450°C, 1500°C and 1550°C have smaller grain sizes than samples produced from commercial zirconia powder (COM).

4.2.6 Mechanical Test Results

4.2.6.1 Microhardness

The microhardness graph of ceramic samples sintered at 1450°C, 1500°C, and 1550°C is given in Fig. 4.18 together with the results obtained. The hardness values of the samples sintered at 1450°C, are in the range of 1365-1046 HV. The OB-145 sample has a lower hardness value of 1315 HV compared to the COM-145 sample. At this temperature, all samples added with recycled zirconia powder, including the 50R-YSZ-145, had a higher hardness value than the COM-145. 100R-YSZ-145 is the sample with the lowest hardness value at 1450°C with 1046 HV.

As seen in the graph, the hardness values of the samples sintered at 1500°C are in the range of 1354-1087 HV. At this temperature, COM-150 had a higher hardness than the OB-150 sample. Adding up to 15% of recycled zirconia powder, including the 15R-YSZ-150 sample, contributed to the increase in hardness values. In the results obtained, the hardness of the mentioned samples is higher than the hardness of COM-150. It was observed that the hardness results of 30R-YSZ-150, 50R-YSZ-150 and 100R-YSZ-150 samples decreased rapidly.

The hardness values of the samples sintered at 1550°C are between 1085-1320 HV. The hardness difference between OB-155 and COM-155 is less at this temperature. Higher hardness results were obtained than COM-155 up to 10% recycled zirconia

powder additive ratio. However, no significant difference was observed between samples 15R-YSZ-155 and 30R-YSZ-155 and COM-155.

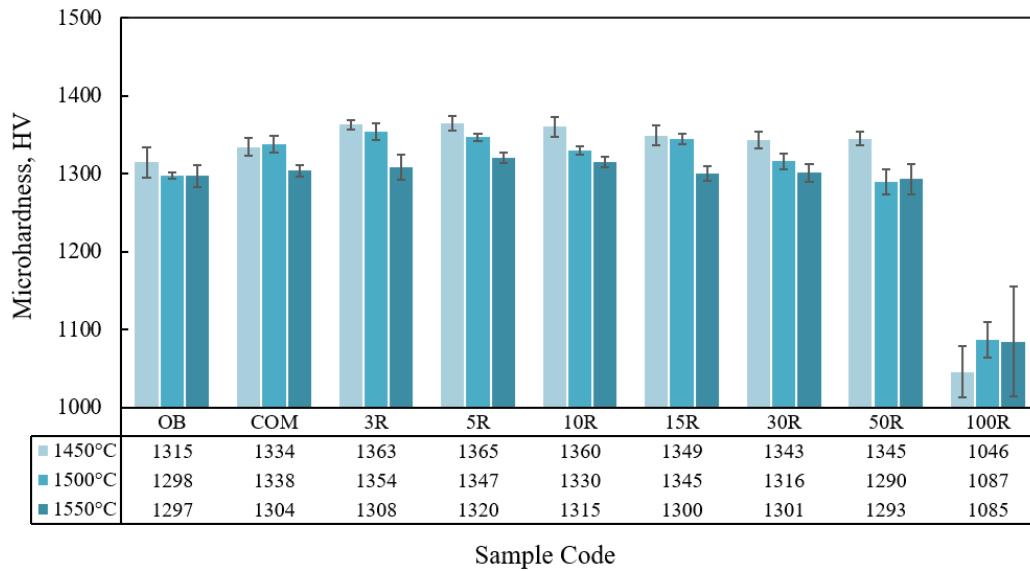


Figure 4.18: Microhardness values of sintered samples

In studies on yttria-stabilized zirconia sintered at different temperatures in the literature, it has been observed that the grain growth, which occurs with increasing sintering temperature and duration time, significantly affects the mechanical properties [64–68]. At the same time, it was stated by Chen et al. [60] that the formation of monoclinic phase in the body affects the mechanical properties negatively. Mago et al. [66] stated that Vickers hardness can be affected by many factors such as existing phases, porosity, grain size, crystal orientation. In this study, when the hardness results of all compositions were evaluated, a significant decrease in hardness results occurred with increasing sintering temperature. Especially, there is a significant decrease in the hardness values of the samples sintered at 1550°C compared to the samples sintered at 1450°C and 1500°C. It has been obtained by experimental results that this situation is caused by grain growth and the monoclinic phase effect that starts to occur at this temperature.

4.2.6.2 Indentation Fracture Toughness

The indentation fracture toughness of ceramic samples sintered at 1450°C, 1500°C, and 1550°C is given in Fig. 4.19 together with the results obtained. Fracture toughness was calculated from the crack lengths produced by Vickers indentations at 10 kgf load. A representative image belonging to the Vickers indentation of sample 5R-YSZ-145 is depicted in Fig. 4.20.

OB-145, 3.55 MPa.m^{0.5} toughness value was the sample with the lowest fracture toughness value at all sintering temperatures. Although an increase was observed in the fracture toughness values of 5R-YSZ-145 and 10-YSZ-145 samples, it can be said that the samples sintered at 1450 degrees have similar toughness values up to 50% recycled zirconia additive ratio, when interpreted considering the standard deviation values. The 100R-YSZ-145 toughness reached a very high value of 5.11 MPa.m^{0.5}. No significant change was observed in the toughness values of the samples sintered at 1500°C compared to 1450°C. Only the 5R-YSZ-150 sample increased by 6% to 4.44 MPa. m^{0.5}.

When evaluated with an overview, the toughness values of all compositions increased with the increase in sintering temperature. This situation can be clearly observed in samples sintered at 1550°C. There was a 32% change in fracture toughness of 50R-YSZ-155 sample. The increasing in toughness values is thought to be due to grain growth. Trunec et al. [69] and Kulyk et al. [68] stated that the larger the size of the tetragonal grains, the greater the tendency to undergo stress-induced transformation into their equilibrium monoclinic structures. They emphasized that the return to the monoclinic structure would result in improved fracture toughness properties. As seen in the XRD analysis results of the samples sintered at 1550°C (Fig. 4.9), the monoclinic phase formed at this temperature confirms the existence of t→m transformation caused by grain growth and the reason for the increase in toughness values.

Trunec et al. [69] also reported in the literature that the fracture toughness values of TZP ceramics containing 3 mol% yttria and having a grain size of approximately 300 nm ranged from 3.0 to 5.8 MPa m^{0.5}. Within the scope of this study, the fracture

toughness of all samples sintered at three different temperatures and added with up to 50% recycled zirconia powder yielded results consistent with the specified values.

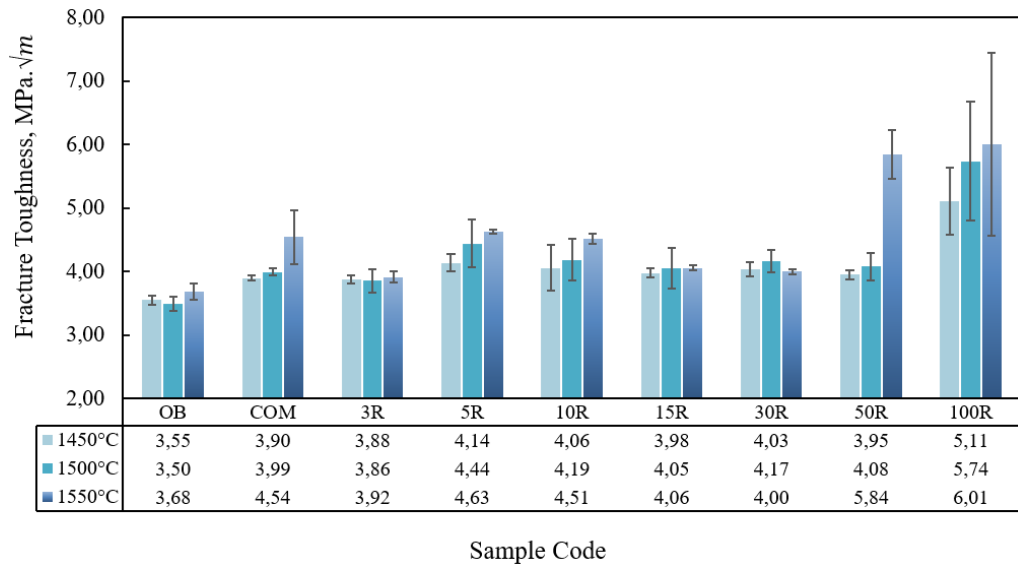


Figure 4.19: Indentation fracture toughness values of sintered samples

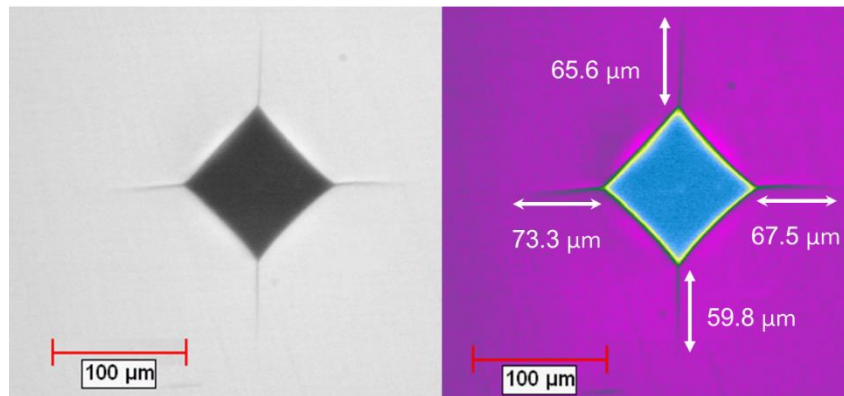


Figure 4.20: Vickers indentation image of 5R-YSZ-145 sample

4.2.6.3 Three-point Bending Test

By evaluating the physical and mechanical properties of the produced samples at different sintering temperatures, the optimum sintering temperature was determined as 1500°C. Three point bending test was applied to all samples except the 3R-YSZ-150 sample which was sintered at this temperature and their elastic modulus was measured

at room temperature. The average of the elastic modulus and three-point bending strength measurement values obtained from three rectangular prism-shaped bar samples produced from each composition. The results obtained are shown in Fig. 4.21.

The elastic modulus of the COM sample was found to be 208 GPa. With the increase of the additive ratio, this value initially decreased, an increase was observed in the 15R-YSZ-150 and 30R-YSZ-150 samples, and the elastic modulus decreased significantly with the further increase in the additive ratio. It has been stated in the literature that the elastic modulus of yttria-doped zirconium oxide is in the range of 200-210 GPa [70–72]. 50R-YSZ-150 and 100R-YSZ-150 samples are below the reported range with their elastic modulus values of 196 GPa and 135 GPa, respectively.

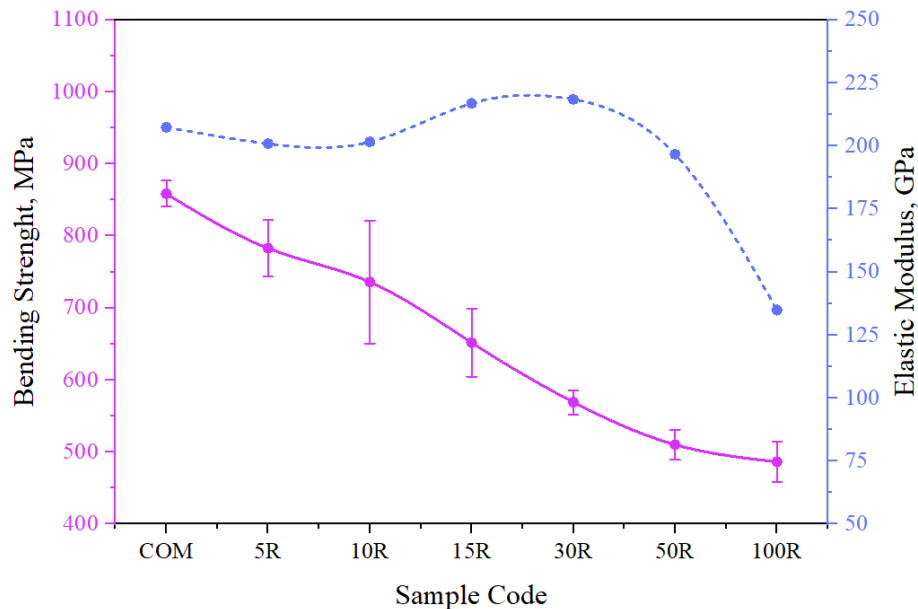


Figure 4.21: Three-point bending strength and elastic modulus curves of all sintered samples

In various studies in the literature, it was observed that the bending strengths of the samples produced from 3 mol% Y_2O_3 ZrO_2 commercial powder were in the range of 800-900 MPa when sintered at temperatures of 1450-1500°C [37,73–76]. When the three-point bending strengths were examined, it was determined that the COM sample had the highest bending strength with 858 ± 18.11 MPa, in accordance with the literature. The bending strength of the samples, which were added with zirconia

recycled from pre-sintered blocks at various rates, decreased with the increase in the additive ratio. The strengths of 5R-YSZ-150, 10R-YSZ-150, 15R-YSZ-150, 30R-YSZ-150 and 50R-YSZ-150 samples were found to be 782 ± 39.26 MPa, 735 ± 85.35 MPa, 651 ± 47.17 MPa, 569 ± 16.94 MPa, and 510 ± 21.18 MPa, respectively. It has been observed that the 100R-YSZ-150 sample, which is made entirely of recycled zirconia, has approximately 50% less strength compared to the COM-150 sample.

Gouveia et al.[37], as a study similar to this thesis study, added 5%, 10% and 50% of recycled zirconia powder to commercial powder in order to determine its potential usage areas and examined the microstructure and mechanical properties of the samples they produced. According to the findings they obtained, as the recycled zirconia powder additive ratio increased, the biaxial flexural strengths of the samples decreased gradually.

Chapter 5

Conclusions

In this master's thesis, the reusability of pre-sintered zirconia blocks, which are wasted after being processed for the production of dental bridges and crowns with CAD/CAM in dental laboratories, was investigated in dental applications. For this purpose, a series of studies were carried out on pre-sintered waste zirconia blocks obtained from dental laboratories and the findings are summarized below.

- 1) Recycled yttria-added dental zirconia powder was mixed with commercial powder in various proportions. A CIP pressure of 250 MPa was applied to the prepared compositions and the ceramic bodies were produced successfully by pre-sintering at 1000°C for 4 hours and then by applying full sintering at 1450°C, 1500°C and 1550°C for 2 hours.
- 2) The bulk density values of all samples after pre-sintering were calculated as 3 gr/cm³, and high densities were obtained with increasing sintering temperature. Taking account of the density value determined by the ISO 13356:2008 standard for zirconia to be used in surgical applications, it was decided that 1450°C were not a sufficient sintering temperature for this study. Considering the standard deviation values, sintering at 1500°C was sufficient up to a maximum of 10% recycled zirconia additive, and the desired densities were reached up to a maximum of 30% additives at 1550°C. The highest theoretical density was reached at maximum sintering temperature, OB-155 and COM-155 samples, 99.2% and 99.4%, respectively. With the increasing recycled zirconia additive, the amount of apparent porosity in the body increased and decreased with increasing sintering temperature.

- 3) The average grain size of the samples sintered at 1450°C, 1500°C and 1550°C was calculated as approximately 0.32 μm , 0.41 μm and 0.56 μm , respectively. According to the ISO 13356:2008 standard, the grain size of the zirconia to be used in surgical applications must be $\leq 0.4 \mu\text{m}$ after sintering. The grain size of the samples sintered at 1550°C was well above the specified values. Therefore, it was decided that the sintering temperature of 1550°C is not a suitable temperature for this study.
- 4) The results obtained from LTD test, clearly demonstrated that the m-ZrO₂ phase percent increased with rising aging time and sintering temperature. Except for 100R-YSZ, all samples sintered at 1500°C demonstrated a considerably high performance after 5 and 10 hours of aging and had less than 25% monoclinic phase percentage in accordance with the characteristics determined by the ISO 13356:2008 standard.
- 5) When all compositions were compared with each other according to the sintering temperatures and additive ratios, it was determined that the hardness values decreased with the increase of the sintering temperature and the amount of recycled zirconia additive, while the toughness values increased. With especially 5R-YSZ, 10R-YSZ, and 15R-YSZ samples, the samples sintered at 1500°C draw attention with their high hardness and fracture toughness values.
- 6) The optimum sintering temperature was determined as 1500°C, considering the density, grain size, phase content, and mechanical performance. According to the three-point bending test results of samples sintered at this temperature, it was observed that the COM, 5R-YSZ, and 10R-YSZ samples gave results consistent with the literature, taking into account the standard deviation values.

In line with this master's thesis, the intended targets have been successfully achieved. In the light of the findings, it is thought that yttria-added zirconia powder, which is recycled from dental blocks, can be reused in dental areas by adding low rates to commercial powder after undergoing the necessary sensitive processes and producing under the determined optimum sintering conditions. Samples with the addition of low proportions of recycled zirconia gave similar or in some cases better results than samples produced entirely with commercial powder in terms of physical and

mechanical properties. These findings are promising in terms of realizing the aims of this study.

Some suggestions are given below in order to improve the obtained results and ensure high efficiency.

- 1) It will ensure that the dust obtained from the waste blocks is passed through a cleaner process, washed with acid and cleaned from the residues and pollutions from the environment. Thus, it may be possible to obtain denser structures, as there will be fewer particles to burn away during the sintering process.
- 2) By working on higher CIP printing pressures and holding times, it can be aimed to obtain denser blocks. More densely packed powders will enable the sintering mechanism to take place at lower temperatures and offer the opportunity to save high energy costs.
- 3) A more detailed study of usability in dental fields should be supported by various test methods, which are important in dental applications, such as color analysis, thermal expansion, optical properties, biocompatibility, chemical solubility.

References

- [1] Murat Mert U. Dental uygulamalara yönelik itriya katkılı zirkonya seramik tozlarının sentezi ve kalıplanabilirlik özelliklerinin incelenmesi (master's thesis). İstanbul: Yıldız Teknik Üniversitesi, 2018.
- [2] Blanchart P. Extraction, properties and applications of zirconia. Industrial Chemistry of Oxides for Emerging Applications, John Wiley & Sons Ltd; Chichester, UK. 2018.
- [3] Nisticò R. Zirconium oxide and the crystallinity hallows. Journal of the Australian Ceramic Society 2021; 57(1): 225–236.
- [4] Nilüfer İB. Atık zirkonya tozlarının değerlendirilmesi (doctoral thesis). İstanbul: İstanbul Teknik Üniversitesi, 2014.
- [5] Alpkılıç DS. Zirkonyanın diş hekimliğinde kullanım alanları. Türkiye Klinikleri J Prosthodont 2017; 3(2): 94–103.
- [6] Holz LIV. Yttria-stabilized Zirconia with beige colour (master's thesis). Universidade de Aveiro, 2017.
- [7] Günhan B. Renkli zirkonya diş bloklarının üretimi ve karakterizasyonu (master thesis). Kütahya: Dumlupınar Üniversitesi, 1986.
- [8] Raza M. Oxygen vacancy stabilized zirconia; synthesis and properties (doctoral thesis). Mons: University of Mons, 2017.
- [9] Phillippi CM, Mazdiyasnı KS. Infrared and raman spectra of zirconia polymorphs. Journal of the American Ceramic Society 1971; 54(5): 254–258.
- [10] Talay E. Üç farklı yttria stabilize zirkonya polikristalinin düşük ısı bozunması

ve bozunmanın materyalin eğilme dayanımına etkisi (doctoral thesis). Konya: Selçuk Üniversitesi, 2015.

- [11] Tarasi F. Suspension plasma sprayed alumina-yttria stabilized zirconia nano-composite thermal barrier coatings–Formation and roles of the amorphous phase. Montreal: Concordia University, 2010.
- [12] Böske TS. Crystalline hafnia and zirconia based dielectrics for memory applications (doctoral thesis). Hamburg: Technischen Universität Hamburg, 2010.
- [13] Kelly JR, Denry I. Stabilized zirconia as a structural ceramic: An overview. *Dental Materials* 2008; 24(3): 289–298.
- [14] Piconi C, Maccauro G. Zirconia as a ceramic biomaterial. *Biomaterials* 1999; 20(1): 1–25.
- [15] Garvie RC, Hannink RH, Pascoe RT. Ceramic steel? *Nature* 1975; 258(5537): 703–704.
- [16] Zhang L, Sun D, Xiong Y, Liu Y. Toughening mechanism and application analysis of ZrO₂ ceramics under high speed strain condition. *IOP Conference Series: Materials Science and Engineering* 2019; 585(1).
- [17] Jitwirachot K, Rungsiyakull P, Holloway JA, Jia-mahasap W. Wear behavior of different generations of zirconia: present literature. *International Journal of Dentistry* 2022: 1–17.
- [18] Garner A, Gholinia A, Frankel P, Gass M, Maclaren I, Preuss M. The microstructure and microtexture of zirconium oxide films studied by transmission electron backscatter diffraction and automated crystal orientation mapping with transmission electron microscopy. *Acta Materialia* 2014; 80: 159–171.
- [19] Claussen N. *Transformation Toughening of Ceramics*, 1987.
- [20] Stevens R. *Zirconia and zirconia ceramics*. Magnesium Elektron Publication; Manschester, UK. .

- [21] Maziero Volpato CA, Altoe Garbelotto LGD, Celso M, Bondioli F. Application of Zirconia in Dentistry: Biological, Mechanical and Optical Considerations. *Advances in Ceramics-Electric and Magnetic Ceramics, Bioceramics, Ceramics and Environment*, InTech; 2011.
- [22] Chevalier J. What future for zirconia as a biomaterial? *Biomaterials* 2006; 27(4): 535–543.
- [23] Chevalier J, Gremillard L, Virkar A V., Clarke DR. The tetragonal-monoclinic transformation in zirconia: Lessons learned and future trends. *Journal of the American Ceramic Society* 2009; 92(9): 1901–1920.
- [24] Lawson S. Environmental degradation of zirconia ceramics. *Journal of the European Ceramic Society* 1995; 15(6): 485–502.
- [25] International Organization for Standardization. ISO 13356:2008(E) Implants for surgery-ceramic materials based on yttria-stabilized tetragonal zirconia (Y-TZP). 2008.
- [26] Keuper M, Berthold C, Nickel KG. Long-time aging in 3 mol.% yttria-stabilized tetragonal zirconia polycrystals at human body temperature. *Acta Biomaterialia* 2014; 10(2): 951–959.
- [27] Arıtman İ. Soğuk izostatik presleme ile üretilen Al/SiCp metal matrisli kompozitlerde faktör etkileşimlerinin mekanik özelliklere etkisi ve karakterizasyon çalışmaları (doctoral thesis). İzmir: Ege Üniversitesi, 2014.
- [28] An Introduction to Cold Isostatic Pressing (CIP). <https://www.sputtertargets.net/blog/an-introduction-to-cold-isostatic-pressing-cip.html> [accessed October 22, 2022].
- [29] Turan E. Investigation of moldability parameters of powder injectionmolded Al-Fe-V-Si composites by adding alumina (master's thesis). Ankara: Gazi University, 2010.
- [30] Tanaka H, Yamamoto A, Shimoyama J ichi, Ogino H, Kishio K. Strongly connected ex situ MgB₂ polycrystalline bulks fabricated by solid-state self-

sintering. *Superconductor Science and Technology* 2012; 25(11).

- [31] Turgut H. Geçiş metali katkılı atık zirkonya esaslı toz karışımlarından sinter seramik malzemelerin geliştirilmesi ve karakterizasyonu (master's thesis). İstanbul: İstanbul Teknik Üniversitesi, 2016.
- [32] Ramakrishnegowda N. Development of layered Mg-Ti composites for biomedical applications (doctoral thesis). Geesthacht: Christian-Albrechts-Universität zu Kiel, 2016.
- [33] Tor C. CAD/CAM sistemleriyle üretilmiş iki yarı saydam, monolitik zirkonya restorasyonun klinik uyumlama prosedürlerinin materyalin optik ve mekanik özelliklerine etkilerinin değerlendirilmesi (doctoral thesis). İstanbul: Biruni Üniversitesi, 2022.
- [34] Sancak Eİ. CAD/CAM materyallerin pürüzlülük, renk ve translusensi özelliklerinin karşılaştırılması (doctoral thesis). Kocaeli: Kocaeli Üniversitesi, 2022.
- [35] Yıldız MF. CAD/CAM ve 3D yazıcılar ile üretilen geçici kronların değerlendirilmesi (doctoral thesis). Kırıkkale: Kırıkkale Üniversitesi, 2022.
- [36] Doğdu C. CAD/CAM ile üretilen seramik kronların marjinal uyum ve mekanik özelliklerinin in vitro olarak değerlendirilmesi (doctoral thesis). İstanbul: İstanbul Medipol Üniversitesi, 2021.
- [37] Gouveia PF, Schabbach LM, Souza JCM, Henriques B, Labrincha JA, Silva FS, *et al.* New perspectives for recycling dental zirconia waste resulting from CAD/CAM manufacturing process. *Journal of Cleaner Production* 2017; 152(January 2019): 454–463.
- [38] Sriboonpeng C, Nonkumwong J, Srisombat L, Ananta S. Effect of vibro-milling time on phase transformation and particle size of zirconia nanopowders derived from dental zirconia-based pre-sinter block debris. *Chiang Mai Journal of Science* 2017; 44(3): 1100–1112.
- [39] Sriboonpeng C, Nonkumwong J, Srisombat L, Pisitanusorn A, Ananta S.

- Influence of sintering temperature on phase formation, microstructure and mechanical properties of the recycled ceramic body derived from CAD/CAM dental zirconia waste. *Chiang Mai Journal of Science* 2019; 46(2): 370–386.
- [40] Iman Jabber Abed and Noor Hashim Abed Al-Manaf. Preparation and characterization of yttria stabilized zirconia blocks from waste dental implant by computer-aided manufacturing (CAM). *Journal of Engineering and Applied Sciences* 2019; 14(8): 10278–10284.
- [41] Silva YBF, Acchar W, Silva VM. Feasibility study of zirconia waste recycling obtained during the machining of single and multiple dental prosthesis. *Materials Science Forum* 2017; 881 MSF: 387–391.
- [42] Kim SS, Lee DY, Seo JI, Bae WT. The properties of sintered body by using the slip casting procesps with remained dental zirconia block after machining. *Journal of Korean Acedemy of Dental Technology* 2012; 34(2): 75–81.
- [43] Cossu CMFA, Pais Alves MFR, de Assis LCL, Magnago R de O, de Souza JVC, dos Santos C. Development and characterization of Al₂O₃-ZrO₂ composites using ZrO₂(Y₂O₃)-recycled as raw material. *Materials Science Forum* 2018; 912 MSF: 124–129.
- [44] Özdoğan MS, Karshoğlu R. Evaluation of microstructure and mechanical properties of PMMA Matrix composites reinforced with residual YSZ from CAD/CAM Milling process. *International Journal of Dental Materials* 2021; 03(02): 37–44.
- [45] Ding H, Tsoi JKH, Kan C wai, Matinlinna JP. A simple solution to recycle and reuse dental CAD/CAM zirconia block from its waste residuals. *Journal of Prosthodontic Research* 2021; 65(3).
- [46] Cordeiro VV, Rodrigues AM, Costa FP da, Cartaxo J de M, Lira H de L, Menezes RR. The harnessing of the waste arising from Y-TZP dental ceramics manufactured by CAD/CAM to be used as alternative dental materials. *Ceramics International* 2022.
- [47] Garvie RC. Patrick SN. Phase analysis in zirconia systems. *Journal of the*

American Ceramic Society 1972; 55(6): 303–305.

- [48] Toraya H, Yoshimura M, Somiya S. Calibration curve for quantitative analysis of the monoclinic-tetragonal ZrO₂ system by X-ray diffraction. *Journal of the American Ceramic Society* 1984; 67(6): 119–121.
- [49] SIST EN 623-3:2002, Advanced technical ceramics - Monolithic ceramics - General and textural properties - Part 3: Determination of grain size and size distribution (characterized by the Linear Intercept Method). 2002.
- [50] Harada K, Shinya A, Yokoyama D, Shinya A. Effect of loading conditions on the fracture toughness of zirconia. *Journal of Prosthodontic Research* 2013; 57(2): 82–87.
- [51] Kök M. Dental zirkonya altyapılar için renklendirme solüsyonlarının üretimi ve karakterizasyonu (doctoral thesis). Kütahya: Kütahya Dumlupınar Üniversitesi, 2020.
- [52] Wiśniewska M, Chibowski S, Urban T, Sternik D. Investigation of the alumina properties with adsorbed polyvinyl alcohol. *Journal of Thermal Analysis and Calorimetry* 2011; 103(1): 329–337.
- [53] Siddaiah T, Ojha P, Kumar NOGVR, Ramu C. Structural, optical and thermal characterizations of PVA/MAA:EA Polyblend films. *Materials Research* 2018; 21(5).
- [54] Surzhikov AP, Ghyngazov SA, Frangulyan TS, Vasil'ev IP, Chernyavskii A V. Investigation of sintering behavior of ZrO₂ (Y) ceramic green body by means of non-isothermal dilatometry and thermokinetic analysis. *Journal of Thermal Analysis and Calorimetry* 2017; 128(2): 787–794.
- [55] Łada P, Miazga A, Konopka K, Szafran M. Sintering behavior and thermal expansion of zirconia–titanium composites. *Journal of Thermal Analysis and Calorimetry* 2018; 133(1): 55–61.
- [56] Hbaieb K. Non-uniform sintering of yttria-stabilized zirconia powder compact. *International Journal of Materials Research* 2015; 106(6): 600–607.

- [57] American Society for Testing and Materials (ASTM) F1873 – 98 Standard specification for high-purity dense yttria tetragonal zirconium oxide polycrystal (Y-TZP) for surgical implant applications. 1998.
- [58] Akimov GY. Cold isostatic pressing as a method for fabricating ceramic products with high physicomechanical properties. *Refractories and Industrial Ceramics* 1998; 39(7–8): 283–287.
- [59] American Society for Testing and Materials (ASTM) C20 - 00, Standard test methods for apparent porosity, water absorption, apparent specific gravity, and bulk density of burned refractory brick and shapes by boiling water. *ASTM International* 00: 20–22.
- [60] Chen F, Wu JM, Wu HQ, Chen Y, Li CH, Shi YS. Microstructure and mechanical properties of 3Y-TZP dental ceramics fabricated by selective laser sintering combined with cold isostatic pressing. *International Journal of Lightweight Materials and Manufacture* 2018; 1(4): 239–245.
- [61] Amat NF, Muchtar A, Amril MS, Ghazali MJ, Yahaya N. Effect of sintering temperature on the aging resistance and mechanical properties of monolithic zirconia. *Journal of Materials Research and Technology* 2019; 8(1): 1092–1101.
- [62] Kosmač T, Oblak Č, Marion L. The effects of dental grinding and sandblasting on ageing and fatigue behavior of dental zirconia (Y-TZP) ceramics. *Journal of the European Ceramic Society* 2008; 28(5): 1085–1090.
- [63] Inokoshi M, Zhang F, De Munck J, Minakuchi S, Naert I, Vleugels J, *et al.* Influence of sintering conditions on low-temperature degradation of dental zirconia. *Dental Materials* 2014; 30(6): 669–678.
- [64] Stawarczyk B, Özcan M, Hallmann L, Ender A, Mehl A, Hämmerlet CHF. The effect of zirconia sintering temperature on flexural strength, grain size, and contrast ratio. *Clinical Oral Investigations* 2013; 17(1): 269–274.
- [65] Dahl P, Kaus I, Zhao Z, Johnsson M, Nygren M, Wiik K, *et al.* Densification and properties of zirconia prepared by three different sintering techniques. *Ceramics International* 2007; 33(8): 1603–1610.

- [66] Mago S, Sharma C, Sharma P, Singh KL, Singh AP. Comparative analysis of yttria stabilized zirconia (YSZ) and titania doped YSZ (YZT) sintered by two different routes: Conventional and microwave processing. *Oriental Journal of Chemistry* 2018; 34(5): 2539–2547.
- [67] Othman SZ, Ramesh S, Teng WD. Sintering of Commercial Yttria-Stabilized Zirconia. *Engineering ETransaction* 2006; 1(2): 14–18.
- [68] Kulyk V, Duriagina Z, Vasylyv B, Vavrukh V, Kovbasiuk T, Lyutyy P, *et al.* The Effect of sintering temperature on the phase composition, microstructure, and mechanical properties of yttria-stabilized zirconia. *Materials* 2022; 15(8): 2707.
- [69] Trunec M, Chlup Z. Higher fracture toughness of tetragonal zirconia ceramics through nanocrystalline structure. *Scripta Materialia* 2009; 61(1): 56–59.
- [70] Soylemez B, Sener E, Yurdakul A, Yurdakul H. Fracture toughness enhancement of yttria-stabilized tetragonal zirconia polycrystalline ceramics through magnesia-partially stabilized zirconia addition. *Journal of Science: Advanced Materials and Devices* 2020; 5(4): 527–534.
- [71] Zhang Y, Lawn BR. Novel zirconia materials in dentistry. *Journal of Dental Research* 2018; 97(2): 140–147.
- [72] Sivanesan S, Ramesh S, Chin KL, Tan CY, Teng WD. Effect of sintering profiles on the properties and ageing resistance of Y-TZP ceramic. *International Journal of Automotive and Mechanical Engineering* 2011; 4(1): 405–413.
- [73] Guazzato M, Albakry M, Ringer SP, Swain M V. Strength, fracture toughness and microstructure of a selection of all-ceramic materials. Part II. Zirconia-based dental ceramics. *Dental Materials* 2004; 20(5): 449–456.
- [74] Ding H, Tsoi JKH, Kan C wai, Matinlinna JP. A simple solution to recycle and reuse dental CAD/CAM zirconia block from its waste residuals. *Journal of Prosthodontic Research* 2021.
- [75] Yilmaz H, Aydin C, Gul BE. Flexural strength and fracture toughness of dental

core ceramics. *Journal of Prosthetic Dentistry* 2007; 98(2): 120–128.

- [76] Li C, Liu Z, Liu G, Ding Y. Experimental investigations of mechanical characteristics and tribological mechanisms of nanometric zirconia dental ceramics. *Open Materials Science Journal* 2011; 5: 178–183.

Curriculum Vitae

Name Surname : Merve TORMAN KAYALAR

Education:

- 2011–2015 Sakarya University, Department of Metallurgy and Materials Science Engineering
- 2019–2022 İzmir Kâtip Çelebi University, Department of Materials Science and Engineering

Work Experience:

- 2019 – 2022 Research Assistant in İzmir Kâtip Çelebi University, Faculty of Engineering and Architecture, Department of Materials Science and Engineering, Department of Materials
- 2022 – 20.. Research Assistant in Gebze Technical University, Faculty of Engineering, Department of Material Science and Engineering, Department of Materials

Papers presented at international scientific meetings and published in proceedings books:

1. **Torman Kayalar Merve**, Yavaş Ahmet, Güler Saadet, Sütçü Mücahit (2021). Effect of Milling on Physical Properties of Zirconia Powders Recycling from Dental Zirconia Based Presintered Block Residuals. 4. International Conference on Materials Science, Mechanical and Automotive Engineerings and Technology (4), 269-269. (Summary) (Control No:7104019).

2. **Torman Kayalar Merve**, Yavaş Ahmet, Güler Saadet, Sütçü Mücahit, Erol Mustafa, Yaraş Ali, Gençel Osman, Erdoğan Ertuğrul (2021). The Self-Cleaning Properties of Zinc Extraction Residue Added Clay Bricks. 4. International Conference on Materials Science, Mechanical and Automotive Engineerings and Technology, 270-270. (Summary) (Control No:7104030).
3. Yavaş Ahmet, **Torman Kayalar Merve**, Güler Saadet, Sütçü Mücahit, Erol Mustafa, Yaraş Ali, Gençel Osman, Erdoğan Ertuğrul (2020). The Photocatalytic Performances of Clay Bricks. 5. International Conference on Material Science and Technology (IMSTEC 2020), 261-261. (Summary) (Control No:6578859).
4. **Torman Kayalar Merve**, Öksüz Kerim Emre, Şen Şaduman, Şen Uğur (2017). Dielectric Properties of Sr-Doped BaZrO₃ Ceramics. 10th International Conference on Materials Science Engineering (Bramat 2017), 907, 21-24, (Full Text) (Control No:6463268).
5. **Torman Kayalar Merve**, Öksüz Kerim Emre, Şen Şaduman, Şen Uğur (2017). The Influence of Composition and Calcination Temperature on the Phases in (Ba_{1-x}Sr_xZr)O₃ Perovskites. 10th International Conference on Materials Science Engineering, 907, 38-42, (Full Text) (Control No:6463104).
6. Öksüz Kerim Emre, **Torman Kayalar Merve**, Şen Şaduman, Şen Uğur (2016). Effect of Sintering Temperature on Dielectric Properties of SiO₂ Doped BaTiO₃ Ceramics. 18th International Conference Materials, Methods Technologies, 10, 361-366. (Full Text Paper) (Yayın No:6463343).

Articles published in national peer-reviewed journals:

1. **Torman Kayalar Merve**, Erdoğan Gökhan, Yavaş Ahmet, Güler Saadet, Sütçü Mücahit (2021). Fabrication of Porous Anorthite Ceramics Using Eggshell Waste as a Calcium Source and Expanded Polystyrene Granules. Journal of Polytechnic, (Control No: 7097379)

Articles published in international peer-reviewed journals:

1. Yavaş Ahmet, Güler Saadet, Onak Günnur, Erol Mustafa, **Torman Kayalar Merve**, Karaman Ozan, Tunç Irmak, Oğuzlar Sibel (2022). Li-Doped ZnO Nanowires on Flexible Carbon Fibers as Highly Efficient Hybrid Antibacterial Structures. Journal of Alloys and Compounds, (Control No: 7160448).
2. Kalkan Şevket Onur, Yavaş Ahmet, Güler Saadet, **Torman Kayalar Merve**, Sütçü Mücahit, Gündüz Lütfullah (2022). An Experimental Approach to a Cementitious Lightweight Composite Mortar Using Synthetic Wollastonite. Construction and Building Materials, 341, 127911 (Control No: 7699700).
3. Yavaş Ahmet, Güneş Fethullah, Erol Mustafa, Sütçü Mücahit, Güler Saadet, **Torman Kayalar Merve**, Keskin Özgür Yasin (2022). Development of Visible Light Active Self-Cleaning Clay Roofing Tiles as Novel Building Materials: An investigation on the Effects of α -Fe₂O₃ Coating and Firing Temperature. Journal of Cleaner Production, 362, 132302 (Control No: 7699713).

4. Yavaş Ahmet, Güler Saadet, **Torman Kayalar Merve**, Sütçü Mücahit, Erol Mustafa, Yaraş Ali, Gençel Osman, Erdoğan Ertuğrul (2021). Effect of Firing Temperature on Self-Cleaning and Photocatalytic Performance of Clay-Based Bricks Under Visible Light Irradiation. Journal of the Australian Ceramic Society, (Control No: 7242413).

Projects:

- 1) CAD/CAM İşleme Prosesinden Elde Edilen Dental Zirkonya Atıklarının Geri Dönüşümü, Project No: 2021-TYL-FEBE-0016, Scientific research project supported by Council of Higher Education, Researcher: **Merve Torman Kayalar**, Executor: Mücahit Sütçü, Project Duration: 04/08/2021-04/08/2022 (National).
- 2) Metal Oksit Katkılı Perovskit Yapılı Ba(Ti,Zr)O₃ Seramiklerinin Üretimi ve Karakterizasyonu, Project No: 2016-01-08-054, Scientific research project supported by Council of Higher Education, Researcher: **Merve Torman Kayalar**, Executor: Şen Uğur, Researcher: Şen Şaduman, Researcher: Öksüz Kerim Emre, Project Duration: 06/12/2016- 06/06/2018 (National).